END

FILMED

DTIC

MICROCOPY RESOLUTION TEST CHART
NATIONAL BUREAU OF STANDARDS-1963-A

AD A124676

USING ARSINE (AsH$_3$) AS A SOURCE OF

ARSENIC IN MOLECULAR BEAM EPITAXY

THESIS

GEP/PH/82-D·5 Gregory C. Clark
Major   USAF

DTIC
ELECTE
FEB 2 2 1983

DEPARTMENT OF THE AIR FORCE
AIR UNIVERSITY (ATC)
AIR FORCE INSTITUTE OF TECHNOLOGY

A

Wright-Patterson Air Force Base, Ohio

83 02 022 152

DTIC FILE COPY

DTIG
COPY
INSPECTED
2

USING ARSINE (AsH$_3$) AS A SOURCE OF

ARSENIC IN MOLECULAR BEAM EPITAXY

THESIS

GEP/PH/82-D-5 Gregory C. Clark
Major   USAF

Approved for public release; distribution unlimited.

USING ARSINE (AsH$_3$) AS A SOURCE OF ARSENIC IN

MOLECULAR BEAM EPITAXY

THESIS

Presented to the Faculty of the School of Engineering

of the Air Force Institute of Technology

Air University

in Partial Fulfillment of the

Requirements for the Degree of

Master of Science

by

Gregory C. Clark, M.S.

Major   USAF

Graduate Engineering Physics

December 1982

Preface and Acknowledgements

By using arsine as a source of arsenic, instead of a solid source, as is the standard practice, I had hoped at the outset, to prove the feasibility of a previously untried method of growing gallium arsenide, by molecular beam epitaxy. I had also been so bold as to hope, that during the short time over which this thesis study was to be conducted, that I would be able to move into the unexplored area of growing AlGaAs using arsine. As the realities of experimental research began to introduce themselves to me in their characteristically persuasive manner, I saw these hopes fade into the approaching autumn. This, notwithstanding, I feel that we, my co-workers and I, have made a not insignificant contribution towards the realization of this goal. It is my trust that this document will be an aid to others who will now pick up the reins.

I am deeply indebted to Dr. Cole Litton, for his untiring efforts both in aspects technical and practical, for his selflessness in time and material, and for his unchanging optimism. My sincere thanks are due also Dr. Donn Shankland, who knew always to be encouraging. I wish to thank also the many others who helped in the construction of the arsine cracking system, and who often provided much needed technical support and encouragement. My special "thank you" goes out to misters: Gene Johnson, Bob Ford, and Don Naas. Also, in particular, to Jimmy Ray, my sincere thanks, for without his very unusual and considerable glass-blowing skills, this project would not have been possible.

I am indebted to Larry Swenk and the many craftsmen who work with him for their help in "manufacturing" parts and equipment used in this project.

My thanks too, to Dr. Peter Colter and Second Lieutenant Larry Kapitan for their many helpful hints and suggestions, and to my loving wife, who did more than her share of listening when I needed to talk.

<div align="right">Gregory C. Clark</div>

iii

Contents

Contents

List of Figures

List of Tables

Abstract

Recent research indicates that cracked arsine produces a better source of As than the conventional solid sources for the MBE growth of quality semiconductors. Further investigation into this topic was the problem of this thesis. A Varian 360 MBE system with conventional furnaces was modified for use with arsine. An arsine handling system and two different cracking furnaces using commercially available resources were constructed. The first furnace constructed was a bulbous design with internal baffles for insuring longer furnace dwell times for the arsine molecules. The second design used a helical quartz tube, approximately 20 inches long, inside a tantalum furnace. Several samples were grown using each cracking furnace. Preliminary results indicate an unsuspected cracking mechanism is responsible for earlier successes; perhaps the primary cracking mechanism is not pyrolytic but photolytic or catalytic.

I. Introduction

Molecular beam epitaxy (MBE) is a process by which multilayer semiconductor crystals are grown under ultrahigh vacuum (UHV) conditions. Successive epitaxial layers or thin films (mainly III-V compounds) are deposited on a semiconductor substrate by controlling the direction and flux of one or more thermal molecular beams. State-of--the-art MBE processes allow for precise control of molecular fluxes and therefore, layer thickness and dopant concentrations. Vacuum conditions (10^{-9} to 10^{-12} Torr) insure atomically clean surfaces are maintained throughout the growth period. And since the atomic and molecular effusion can be switched on or off by means of a shutter, rapid changes of beam species can be realized, and excellent control of crystal stoichiometry can be achieved by careful adjustment of specie beam flux.

Practical applications for MBE-grown crystals are numerous. Possible uses include very high speed integrated circuits (VHSIC's), IMPATT diodes, varactors, Schottky barrier FET's, optical waveguides, high speed (in the pico-second range) switches, negative affinity photocathodes, solid state injection and diode lasers, very large scale integrated circuits (VLSIC's), etc. See Table I. MBE's most significant applications are those in which it is critically important that crystalline layers are ultrathin or have sharp doping profile variations, as well as extremely sharp heterojunction interfaces in semiconuctor layers.

The increasing demand in electronic technology for thin layer, extremely high electron mobility devices with carefully controlled doping profiles makes the MBE process one of intense interest.

1

TABLE I

SEMICONDUCTOR DEVICES MADE FROM MBE LAYERS (Ref 13)

MATERIAL	DEVICE	INITIAL RESULTS	REFERENCE
GaAs-Al$_x$Ga$_{1-x}$As	DH LASER	CW UP TO 400°K, I$^{th}_{300K}$=3.3 10^{3}A/cm^2	CHO,DIXON,CASEY, HARTMAN
GaAs	FET	NOISE FIGURE = 1.9 dB, ASSOCIATED GAIN = 11 dB-6 GHz	CHO,DILORENZO,HEWITT, NIEHAUS,SCHLOSSER
GaAs	MIXER DIODE	CONVERSION LOSS 5.3dB 51.5 GHz, 8.5dB 103 GHz, CUT OFF FREQ. = 500 GHz	BALLAMY,CHO
GaAs	IMPATT DIODE	LO-HI-LO PROFILE, POWER = 3.2 W 11.7 GHz, EFF. = 18%	CHO,BALLAMY,DUNN, KUVAS,SCHROEDER
GaAs-Al$_{0.3}$Ga$_{0.7}$As	INTERFERENCE FILTERS QUARTER WAVE STACKS	BANDWIDTH 300 – 900 Å, 15 LAYER REFLECTANCE 1.5μm>99%	VANDERZIEL,ILEGEMS
Al$_x$Ga$_{1-x}$As	WAVEGUIDE	LOSS$\leq$1.5 cm^{-1}(0.89-1.1 μm)	MERZ,CHO
GaAs-Al$_x$Ga$_{1-x}$As	TAPERED COUPLER	EFFICIENCY = 100%	MERZ,LOGAN,WIEGMANN, GOSSARD
PbTe-Pb$_{0.78}$Sn$_{0.22}$Te	DH LASER	CW UP TO 114°K, TUNABLE FROM 8.54 TO 15.9 μm	WALPOLE,CALAWA, HARMAN,GROVES
PbTe-Pb$_{0.88}$Sn$_{0.12}$Te	WAVEGUIDE	LOSS < 1.5 cm^{-1}(10.6 μm)	RALSTON,WALPOLE, HARMAN,MELNGAILIS
PbTe-Pb$_{0.78}$Sn$_{0.22}$Te	DFB LASER	CW UP TO 50°K, SINGLE MODE TUNING = 7 cm^{-1}	WALPOLE,CALAWA, CHINN,GROVES,HARMAN

Historical Background

The history of the MBE process shows it to be essentially a refinement of earlier evaporation growth techniques first described by Guenther (Ref 1,2). Guenther's so-called three-temperature method used two evaporating sources and a substrate, each at a different temperature. The introduction of elemental beams and UHV conditions by Arthur and Lepore and extensive refinements by Cho provide the basis for today's MBE systems (Ref 3,4). In 1968, in a simple quartz-pyrex vacuum system, John Davey and Titus Pankey of the Naval Research Laboratory (NRL) were the first to grow gallium arsenide (GaAs) by MBE, (Ref 5). The main difference between MBE and Guenther's three-temperature technique is, that in MBE, the sources are focused molecular or atomic beams whose fluxes can be carefully controlled.

When compared with vapor phase epitaxy (VPE), the MBE process is still unable to achieve the high mobilities common to VPE, but continued improvements in this area seem certain. The basic approach to vapor phase epitaxial growth of GaAs is to pass arsenic trichloride over a hot gallium boat using hydrogen as a propellant gas. This is why it is sometimes called the "hot wall" growth technique. The resultant chemical reaction favors gallium arsenide with only a small variation in the gallium to arsenic ratio; in other words, the stoichiometry of the crystal can not be adjusted as is possible in MBE. Because of the chemical reaction involved, VPE provides no convenient means for the growth of ternary and quarternary crystals. VPE is, however, one of the most reliable and widely used methods of growing relatively thick semiconductor crystals.

3

Yet another method of growing GaAs is a process called metal
organic chemical vapor deposition (MOCVD) or alkyl chemical vapor
deposition. This method employs trimethyl-gallium, $(CH_3)_3Ga$, or
triethyl-gallium, $(CH_3-CH_2)_3Ga$, reacting with a gaseous mixture of
5% arsine (AsH_3), and 95% hydrogen. This reaction produces GaAs on
the cool walls of the growth chamber, thus MOCVD is known also as a
"cold wall" growth technique.

MOCVD offers some of the advantages of MBE, such as uniformity of
crystal growth, control of crystal stoichiometry, possible use for
growing ternary and quarternary compound crystals, etc. However, it
also shares the disadvantage of lower electron mobilities, when compared
with crystal samples grown by vapor phase epitaxy. MOCVD crystals have
also a major disadvantage when compared to crystals grown by the MBE
process; namely, MOCVD crystals show high carbon contamination levels.
Although carbon contamination is a problem in MBE, it is not nearly as
severe as in alkyl crystal growth. This is true because the only
possible source of carbon contamination in the ultra high vacuum system
of the MBE process, (unless graphite crucibles are used) is residual
carbon in compound with other elements in the MBE growth chamber. These
contaminants can be inadvertently captured during growth of the crystal,
a fact which can seriously degrade the quality of the semiconductor. In
the MOCVD process, however, carbon in compound with hydrogen is an
active participant in the chemical reaction. Therefore, carbon
contamination is more prevalent.

Among the most commonly grown crystals using the MBE method are
multilayered crystals known as superlattices. A typical example is thin
aluminum-gallium-arsenide layers with alternating layers of gallium

4

arsenide (AlGaAs/GaAs), where the layer thicknesses are typically in the range of a few hundred to a few thousand angstroms.

Historically, GaAs crystals and AlGaAs/GaAs superlattices have been grown by MBE using solid arsenic sources. Recent studies show however, that the use of arsine (AsH_3) as the arsenic source offers further improvements in the purity·and electrical character of the GaAs crystals (Ref 6). Using gaseous AsH_3, separated into its constituent parts by means of a cracking furnace in the UHV chamber, Calawa and his associates have produced GaAs layers of higher purity and electron mobility than any previous samples grown by MBE using solid arsenic (Ref 7).

The reasons for the improved purity and electron mobility are not fully understood, but it is believed that the As_2 and As_4 polymers formed when using solid arsenic are not as conducive to high quality growth as is the As_1 which results from cracking AsH_3. It is also unclear exactly what role the liberated hydrogen plays in the enhancement of crystal quality, but it seems to exhibit a positive influence as a reducing agent for other impurities.

Statement of the Problem

The central problem of this thesis is to further study the use of arsine gas instead of solid arsenic in growing gallium arsenide crystals by MBE. In as much as possible, during the short time over which this study extends, advantages and disadvantages of using arsine have been investigated. Some of the disadvantages immediately present themselves. Since arsine is an extremely poisonous gas, extra precautions such as the use of portable breathing units and an all-welded stainless steel construction have been necessary to insure the gas is handled safely

5

during all phases of the project. Extra equipment was required to transform the arsine in a precisely controlled amount from the liquid state in which it is provided in a pressure tank, first to a gaseous molecular state and then to a cracked atomic state in which it is useful in the MBE chamber, (see Chapter III). Expected advantages are higher purity crystals with increased electron mobility, and thus enhanced capabilities for semiconductor devices.

II. Theoretical Considerations

The scope of this study could not possibly deal with the fundamental physics that are pertinent to the field of crystal growth and characterization. Nor does time or space permit the in-depth treatment of any one of the myriad subjects relating to MBE growth. It is left then, to briefly introduce in this chapter some of the subject matter of primary importance.

In this chapter we will briefly describe Knudsen cell effusion as it relates to the use of solid sources in the MBE system. Appendix A shows some data which is pertinent to Knudsen cell effusion in growing GaAs. This chapter will also serve to introduce band theory and to illustrate the band structure of GaAs in the region of the zone-center of the first Brillouin zone. Two other important aspects of crystal growth, sticking coefficients and lattice matching, will be briefly outlined as well.

The second portion of this chapter will be devoted to a brief description of the in situ analysis of the as-grown epitaxy, i.e. Auger electron spectroscopy (AES) and mass spectrometry. Although, they are by no means the only methods used to evaluate the crystal while it is still under the UHV of the growth chamber, they represent two of the most widely used in situ analysis techniques.

The third and final thrust of this chapter will be in the area of crystal characterization. Hall-Effect measurements, capacitance-voltage (C-V) profiling, and photoluminescence will be summarized.

7

Knudsen Cell Effusion

An expression for the number of molecules per unit time that will strike a unit area of a container can be derived from fundamental considerations in gaseous thermo-dynamics (Ref 8). Also the related question of how many molecules per unit time will escape through a small orifice in the container, is generally approached in this manner. This derivation then, will give us an approximate expression for the flux of molecules impinging on a substrate from a Knudsen cell oven.

We first consider an element of area dA on the wall of the container and ask how many molecules will strike this area in time dt? We can see that those molecules whose velocity is between v and v + dv and whose direction with respect to the normal of the area is θ will move a distance vdt in time dt. And if we only consider those moving toward dA, then we can see that only the molecules inside this infinitesimal cylinder of volume dA vdt cos θ will strike the wall in time dt. Molecules outside this cylinder will not.

If f(v) is the distribution function for the molecules inside the cylinder, then the number of molecules per unit volume in this velocity range is $f(v)d^3v$. Thus, the number of molecules in this volume which strike the wall is $[dA \ vdt \ \cos θ][f(v)d^3v]$. We now divide this by dAdt and obtain the flux, , the number of molecules with velocity between v and v + dv that strike a unit area, which is given by

$$\phi(v)d^3v = d^3v \ f(v) \cos θ \qquad (1)$$

Now, if we sum over all speeds between zero and infinity and over all angles from zero to 2π, (we must do this twice since azimuthal

8

angles must also be considered) we will have the total number of mole-cules which strike the unit area in unit time, Φ_o. Changing to spherical coordinates and performing the integration we get

$$\Phi_o = \pi \int_0^\infty f(v)v^3 dv \qquad (2)$$

Expressing this in terms of the mean speed of the molecules, v_{ave}, and since $v_{ave} = [4\pi/n]\int_0^\infty f(v)v^3 dv$, we arrive at

$$\Phi_o = \tfrac{1}{4}nv_{ave} \qquad (3)$$

Now, since the equation of state gives us $p = nkT$ or $n = p/kT$, and since the mean speed is given by $v_{ave} = [8kT/\pi m]^{\frac{1}{2}}$, we can combine these results with equation (3) to yield

$$\Phi_o = p/[2\pi mkT]^{\frac{1}{2}} \qquad (4)$$

which is the basic equation used for calculating the flux from a Knudsen cell oven. The units here are molecules $cm^{-2}sec^{-1}$, p and T are the average pressure and temperature inside the cell, m is the mass of the effusing species, and k is Boltzmann's constant.

It is important to note the conditions under which true effusion takes place as opposed to hydrodynamic flow. The condition which must be met is that the diameter of the orifice, D, must be small enough so that there is no appreciable effect on the equilibrium of the gas inside the chamber. In general, the dimensions of the cell must be small compared to the mean free path of the gas molecules. In particular, the

9

diameter of the cell aperture, D, must be small compared to the mean free path, λ. Of course, in the UHV of the MBE chamber, the mean free path of a molecule in a Knudsen cell increases greatly, so D may be increased without disturbing the conditions for effusion, (Ref 8). For example, at ordinary effusion pressures in an MBE system (10^{-6} to 10^{-7} Torr) the mean free path·is more than a meter long.

If equation (4) is modified to account for the distance from the effusing source to the substrate, L, and the area of the aperture, a, it becomes,

$$\Phi_0 = pa/[\pi L^2 (2\pi mkT)^{\frac{1}{2}}] \quad \text{molecules/cm}^2\text{sec} \qquad (5)$$

Because a large mass transfer rate is needed, it is, in practice, inconvenient to use true Knudsen cells. It has been repeatedly demonstrated, however, that the crucibles used in the MBE system described in Chapter III, do approximate Knudsen cell effusion, and practical rates of mass transfer required for crystal growth can be achieved.

The Energy Bands of GaAs and AlGaAs

The general approach to understanding electronic motion in a crystal is to solve the Schroedinger equation for a single electron in a one dimensional periodic potential (Ref 9). The solutions then take the form of Bloch functions (Ref 10,11). It is from this treatment that the well-known energy bands of a crystalline lattice and the energy levels due to impurities evolve. The band structure of a given semiconductor is of great importance when studying the optical and electrical characteristics of the material. Figure 2-1 shows a typical energy, E,

versus wave vector, k, diagram for the region near the center of the
first Brillouin zone for GaAs. For AlGaAs structures, up to concen-
trations of $Al_{.4}Ga_{.6}As$, the band diagram is only slightly changed from
that shown in Figure 2-1. As the concentration of aluminum is increased
above .4 levels, the semiconductor goes from a direct gap material to an
indirect gap semiconductor, i.e. the gap increses faster at the gamma
point than it does at the L point. Figures 2-2 and 2-3 are a schematic
representation of a modulation doped AlGaAs superlattice, and its
conduction band edge diagram respectively. Table II summarizes some of
the important characteristics of GaAs, Si, and Ge for purposes of
contrast and comparison (Ref 12).

Sticking Coefficients

Growth on the substrate is determined to a large extent by the
sticking coefficients or surface lifetimes for the molecules in the beam
flux. To some extent this is also true of the impurities in the MBE
system. For an assumed sticking coefficient of unity, Calawa estimated
that for the highest growth rates, (3-10 Angstroms/sec) a vapor pressure
of 10^{-15} Torr would be required to keep unwanted impurities at a level
of $10^{14}/cm^3$ (Ref 13). This means, at a vapor pressure in the
10^{-10} Torr range, impurity gases strike the surface at about 10^{-3}
times the gallium flux (Ref 13).

For growth of the desired species it was first estimated that the
adsorption and desorption or lifetime of Ga atoms is characterized by
the constant τ, which is related to the temperature T by:

$$\tau = 2.5 \times 10^{-15} \exp[2.61 \pm .17 eV/kT] \text{ with Ga on [111]} \quad (6)$$

11
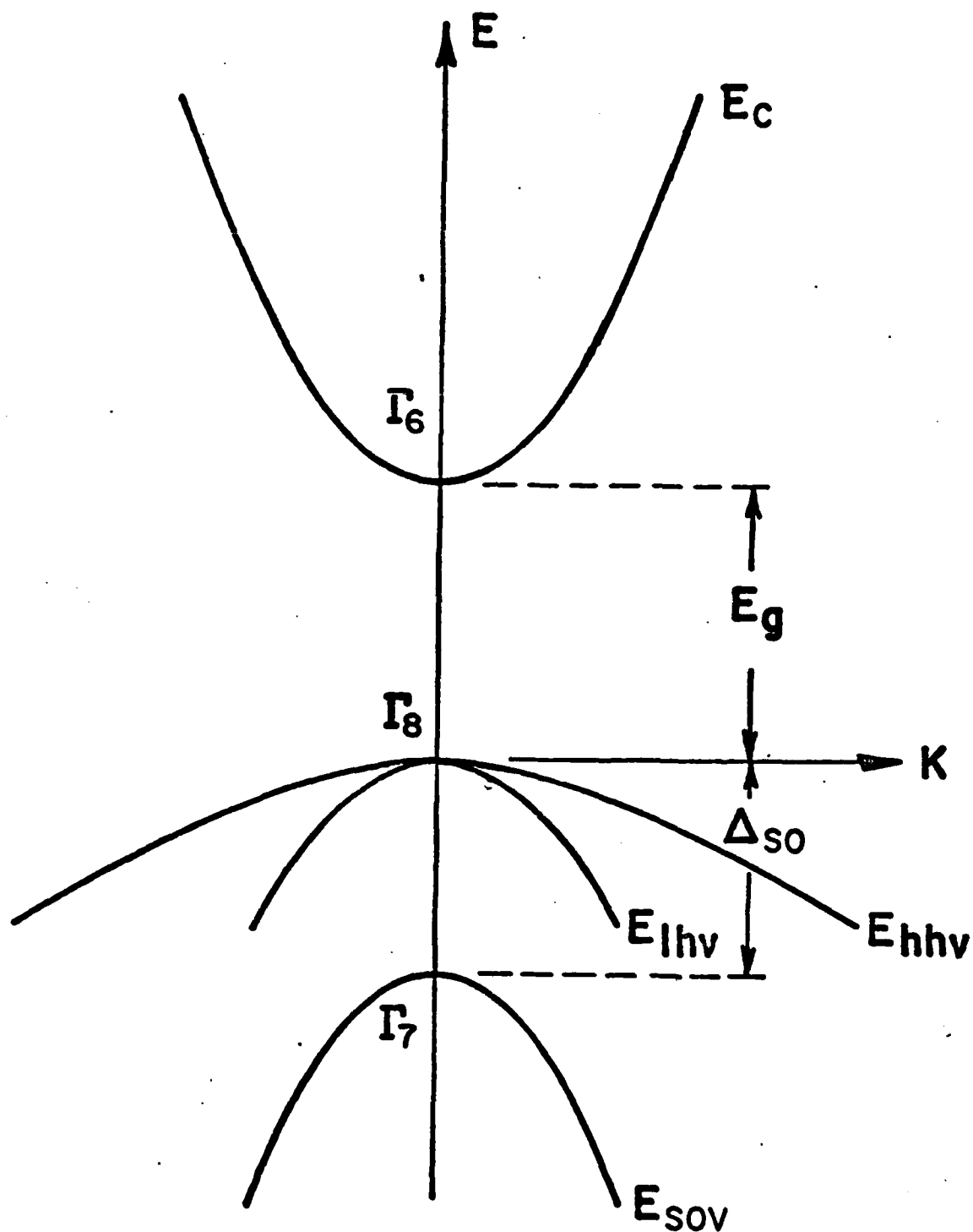
Energy Bands of GaAs at K=0 (Zincblende Cubic)
E_g=1.5196 eV, Delta$_{so}$=0.34 eV

Figure 2-1 Band Structure of GaAs

12

GaAs (1200 Å)

Undoped

Si Doped

Undoped

(Al,Ga) As

GaAs (1000 Å)

Ga As Buffer Layer

GaAs (10 μm)

Si Substrate
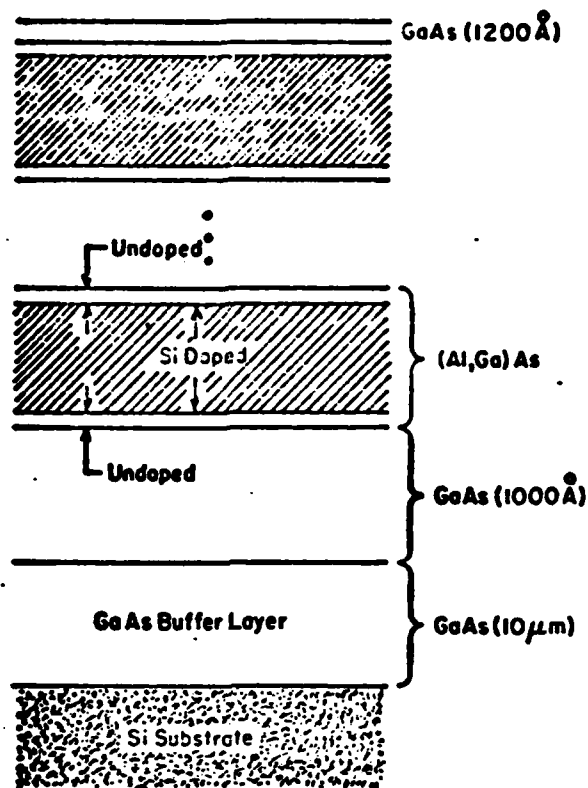
Figure 2-2 Schematic Representation of Modulation Doped AlGaAs/GaAs

Ionised Donors

Doped

Undoped

Fermi Level

GaAs Undoped

(Al,Ga)As

GaAs Surface Layer (~200Å)

Two-Dimensional Electron Gas
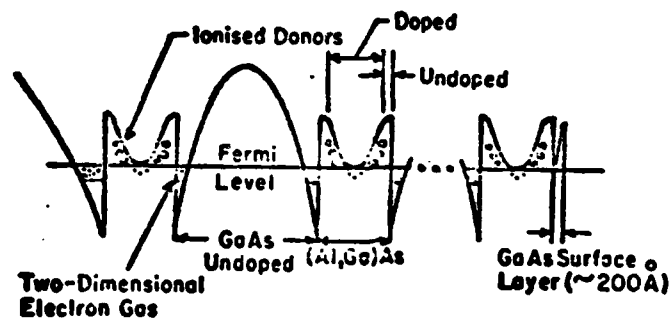
Figure 2-3 The Conduction Band Edge Diagram of AlGaAs/GaAs

13

TABLE II

IMPORTANT ELECTRONIC PROPERTIES OF SEMICONDUCTORS (Ref 12)

* Temperature 27°C	Ge	Si	GaAs
Energy gap (ev)	0.67	1.1	1.4
Effective density of states (cm^{-3})			
conduction band N_c	1.04×10^{19}	2.8×10^{19}	4.7×10^{17}
valence band N_v	6.0×10^{18}	1.04×10^{19}	7.0×10^{18}
Intrinsic carrier concentration n_i (cm^{-3})	2.4×10^{13}	1.45×10^{10}	$\sim 9 \times 10^{6}$
Lattice (intrinsic) mobilities ($cm^2/vsec$)			
electrons	3900	1350	8600
holes	1900	480	250
Dielectric constant	16.3	11.7	12
Breakdown field (v/μ)	~ 8	~ 30	~ 35

14

where τ is the average time the gallium atoms stay on the substrate (Ref 14). Below 750°K (477°C) the Ga sticking coefficient was found to be unity. When the As_2 species were studied, it was found that at temperatures above 500°K (227°C) measurable sticking only occurred in the presence of excess gallium atoms on the substrate surface. The conclusion reached was that arsenic could only be adsorbed on the GaAs substrate if it reacts with gallium atoms. So, for stoichiometric growth it is necessary and sufficient to apply an excess of arsenic. We see then that the growth rate is determined solely by the Group V element, Ga (Ref 3). The commonly used ratios of As to Ga using solid arsenic sources are on the order of ten to one.

Lattice Matching

In the growth of an epitaxial layer on a substrate, it is important that the lattice constants of adjoining layers be well matched. This is true also for multiple epitaxial layers such as $Al_xGa_{1-x}As/GaAs$. If the lattice constants of adjoining layers are not closely matched, dislocations or other defects and imperfections will occur at the interfaces and in the as-grown epitaxy. These defects can then lead to optical scattering and unwanted electron-hole recombination (Ref 15). Lattice mismatch may also be responsible for the rapid degradation in the operation of certain heterostructure devices. This is especially true in optical semiconductor devices, such as heterojunction lasers and light emitting diodes (Ref 16). Figure 2-4 illustrates the lattice constant and band gap for some group III-V compounds.
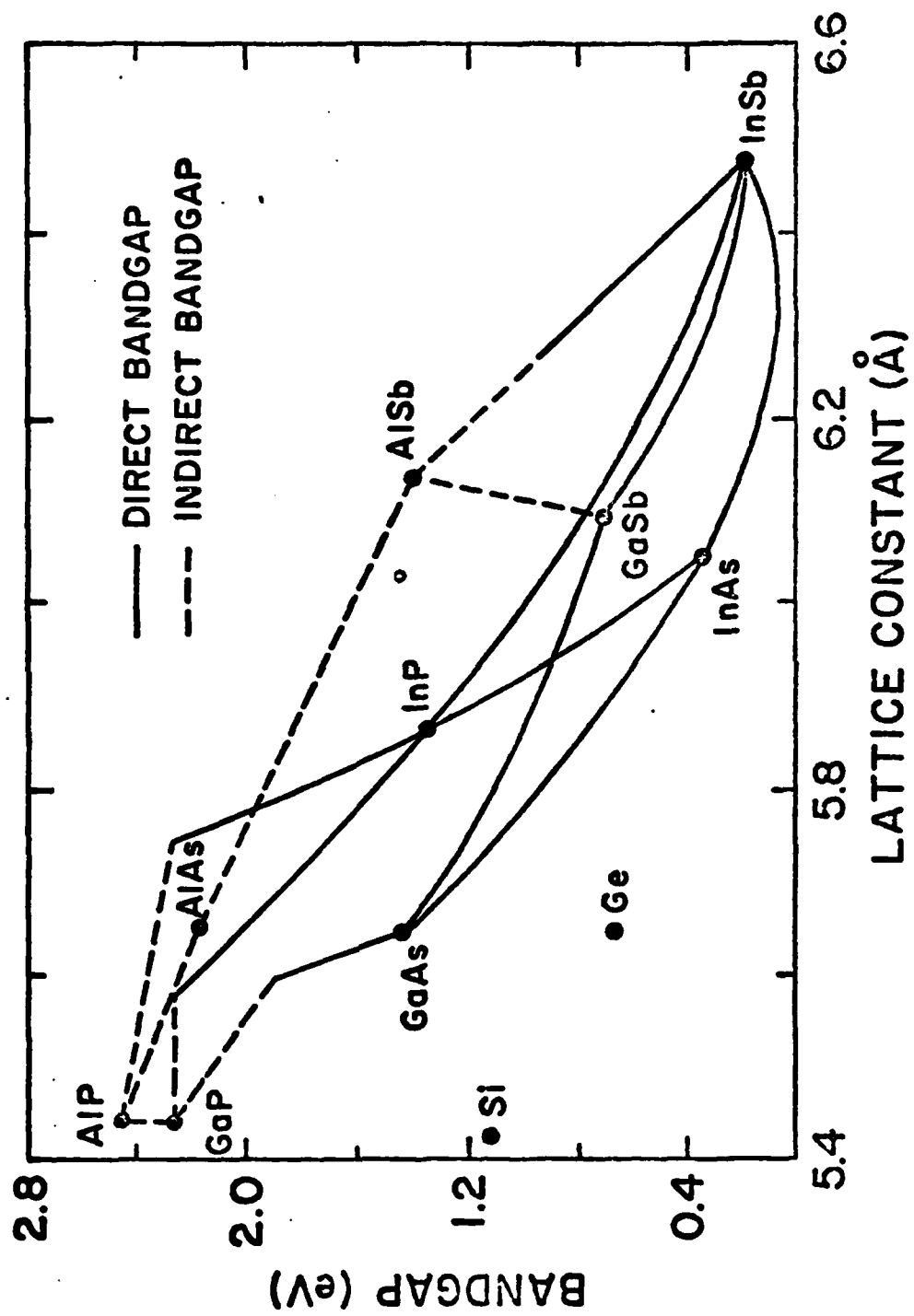
Figure 2-4 Lattice Matching

In Situ Analysis

One of the distinct advantages the MBE process has over the more traditional methods of crystal growth is the extent to which the sample can be analyzed in the UHV growth environment. Numerous techniques are used to analyze the sample in situ. They include: 1) Auger Electron Spectroscopy, (AES); 2) Low-Energy Electron Diffraction, (LEED); 3) Reflection Electron Diffraction, (RED); 4) Mass Spectroscopy; 5) Secondary Ion Mass Spectroscopy, (SIMS); 6) Reflection High Energy Electron Diffraction, (RHEED); and 7) Ellipsometry measurements. Of these techniques only AES with cylindrical mirror analyzer (CMA) optics and a mass spectrometer were available in the MBE system described in this paper.

Auger Electron Spectroscopy. AES is a method of substrate or epitaxial surface analysis. It uses secondary electrons emitted by a surface which was bombarded by a primary electron beam of 1-9KeV energy to determine the chemical composition of the first few layers of atoms on the surface. The primary electron beam ionizes a core level of a surface atom. This ionized atom may then decay to a lower energy state via an electronic rearrangement which leaves the core atom doubly ionized. The energy of the ejected Auger electron represents the difference between these two energy states, and is characteristic of the parent atom. Provided the ejected Auger electron is near the surface it escapes from the surface with little or no loss of energy. In this way the composition of the surface can be determined with relative precision. Thus AES is of great importance in analyzing substrates before and after the MBE growth. The Auger spectrum is the differentiated energy distribution function, $dN(E)/dE$. Its ability to properly detect

17

a given element depends on the possible presence of other interfering elements, the distribution and depth of the element on the surface, the electron beam energy, etc. AES is clearly not greatly useful in detecting deep impurity levels or bulk dopant concentrations (Ref 17); but it is a very sensitive surface analytical tool capable of detecting single monolayers of adsorbed atoms on the surface of a semiconductor or metal.

Mass Spectroscopy. Although the quadrupole mass analyzer was the primary instrument used in analyzing the gases extant in the UHV of the MBE system, several important factors about its use must be considered (Ref 18).

1) Since the quadrupole mass analyzer operates by ionizing an atom or molecule and measuring its mass to charge ratio, it does a certain amount of cracking itself. Therefore this additional cracking must be considered when interpreting data concerning the efficiency of a cracking furnace installed in the system.

2) Since different molecules have different electron configurations in their outer shells, the probability that a thermal electron will remove an electron (or electrons) is different for each molecule. This is known as the ionization coefficient. In general, a molecule's ionization coefficient is proportional to the number of electrons in the molecule.

3) The mass filter transmission coefficient for a molecule is a measure of a molecule's likelihood of being able to pass through the mass analyzer's filter. Lighter molecules pass through this filter more easily than heavier ones and therefore they are more easily detected. For example, As_2 is only 50% as likely to be detected as a lighter

molecule like H_2O; and it (As_2) is fifty times more likely to be detected than As_4.

4) The electron multiplier gain is, in general, proportional to the inverse square root of the mass, so this factor, too, must be reckoned with when computing partial pressures, etc.

Each particular species of gas has its own particular fragmentation or cracking pattern. Unfortunately, not very much is known about the cracking patterns of arsine (Ref 19). Other caveats for using the quadrupole mass analyzer include other unknowns such as: reactions produced by the hot filament, ion-molecule interactions, gas accumulation or trapping rates, etc.

The basic sensitivity, S_B, of the mass analyzer used was given by the factory as 1.5×10^{-3} amps/Torr. When using the Faraday cup the partial pressure, pp in Torr can be calculated from the following:

$$pp = \text{Faraday cup current}/ S_B \qquad (7)$$

In general, the partial pressure for any mass number, m, is determined using the following formula:

$$pp = [EMC/(S_B \times EMG)]m \qquad (8)$$

where EMC is the electron multiplier current and EMG is the electron multiplier gain. For further accuracy, corrections for S_B, gain, background, and transmission are necessary (Ref 20).

19

<u>Characterization Techniques</u>   Although there are numerous techniques

for the characterization of semiconductor growth, only three will be

briefly discussed: Hall-Effect Measurements, C-V profiling, and

Photoluminescence.

   <u>Hall-Effect Measurements.</u> In the absence of an applied field

electrons move about in the semiconductor with a random drift velocity

due to the collisions of thermal heating. This results, however, in no

net displacement of the electrons over long periods because the drift is

purely random. If an electric field is applied, a new, nonrandom

velocity is superimposed on the thermal motion of the carriers in the

sample. This drift velocity, v_{drift}, will cause the electrons to move

in a direction opposite the applied field, E_f. In a similar manner, an

applied magnetic field changes the drift velocity of the electrons in

the sample. The combined effects of applied electric and magnetic

fields, together with thermal gradients give rise to·the so-called

galvanomagnetic effects. The most important of the galvanomagnetic

effects is the Hall effect.

   When current flows in a semiconductor in the x-direction, and a

magnetic field is applied in the z-direction, an electric field is

produced in the y-direction. See Figure 2-4. An electron then, moving

with velocity v_x, experiences a downward Lorentz force, F_y. But, in

equilibrium there can be no net forces acting on the electron; so as a

result, an excess of electrons builds up at the right side of the sample

until their induced electric field balances the Lorentz force, i.e.

$F_y=0$. It is this induced field measurement in a given magnetic field

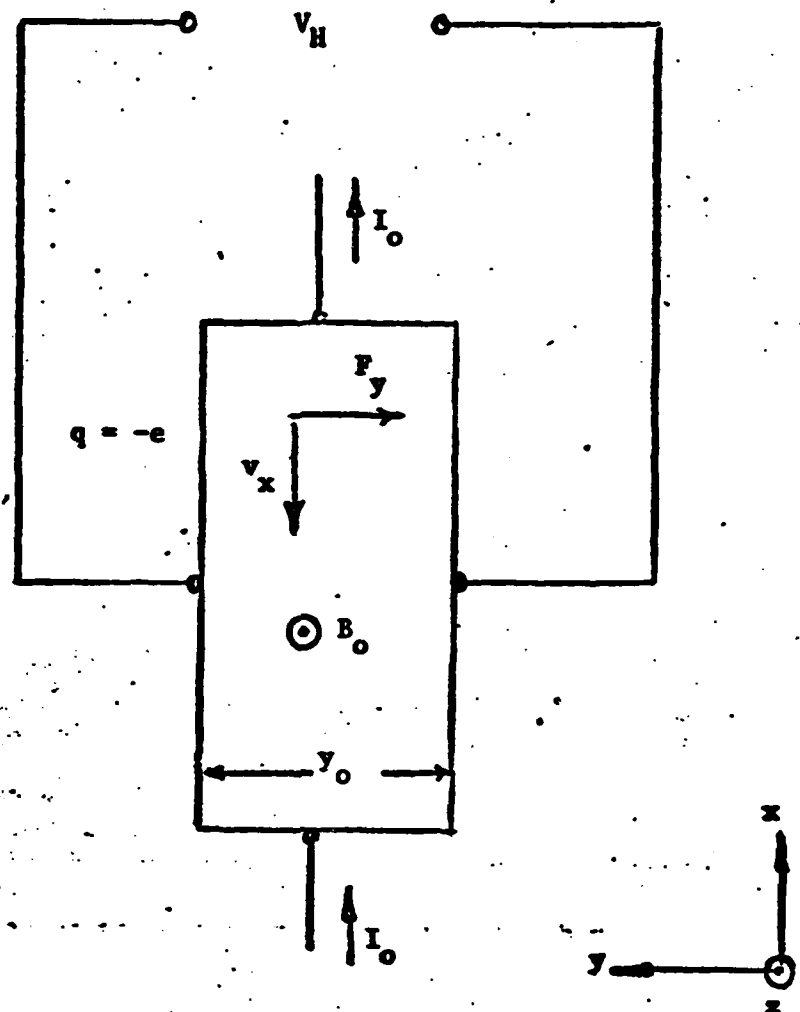that is of primary importance in Hall measurements.

Figure 2-5 Hall-Effect Measurements

In the case where the conductivity of the sample is dominated by only one type of carrier then a simple Hall-Effect analysis is sufficient. The appropriate equations are well known, and give results for the mobility of the carriers, their concentration, and the dopant type, i.e., p or n. See Appendix B.

C-V Profiling. Capacitance-Voltage profiling is a technique whereby the variation of capacitance with applied voltage is used to provide information about the semiconductor such as: the type of semiconductor (p or n), and the depth and the number of carriers in the sample.

Capacitance per unit area can be defined as $C=dQ/dV$, where dQ is the incremental change in charge for an incremental change in voltage dV. In a given semiconductor with an arbitrary impurity distribution, any change in the voltage applied will cause a corresponding change in the measured charge and in the capacitance. This change in capacitance can be related to a change in the width, W, of the depletion region of the semiconductor. $C=Ke/W$, where K is the dielectric constant of the semiconductor and e is the permittivity of free space, 8.86×10^{-14} f/cm = 55.4 e/vμ , (Ref 21).

Photoluminescence. An optically-excited semiconductor emits radiation called photoluminescence. It arises principally from the recombination of electrons and holes bound to the acceptors or donors of the crystal. There are five main types of recombination radiation observed: 1) free electrons recombining with bound holes; 2) free holes with bound electrons; 3) bound electrons with bound holes; 4) the recombination of electron-hole pairs called exitons; and 5) the recombination of exiton complexes which are free exitons bound to impurities or

22

defects. Other recombinations do, in fact, occur but their photoluminescent spectra are so weak, they are often neglected.

At very low temperatures each impurity in the semiconductor sample has its own characteristic photoluminescent "fingerprint". Not only is it possible to accurately identify the impurity in question, but a wealth of additional information about the impurity as well, such as its charge state and position in the lattice, etc. (Ref 22).

III. Equipment

This chapter will first describe, in general, the MBE equipment which comprises the Varian 360 MBE system. Next, in a separate section, those portions of the system which deal with handling arsine from its liquified state in the metal cylinder to the cracking furnace inside the UHV chamber will be described in detail.

The Varian MBE-360 System

The Varian MBE-360 system has five subsystems: vacuum system, source configuration, substrate handling, epitaxy control, and surface analytical instrumentation (Ref 23).

Vacuum System. The vacuum pumps and chambers of the MBE 360 system were designed not only to be capable of producing ultra high vacuum conditions but also to be non-contaminating and to be·compatible with the reactive materials used in the growth process.

The vacuum chamber is a series of interconnecting stainless steel cylinders of various diameters, either welded, using tungsten inert gas welds, or connected together by means of bakeable flange gaskets. The primary chamber, where the MBE growth takes place, is an 18" diameter cylinder (bell jar) into which the sample is brought by means of a laterally-located load lock and positioned by an overhead sample manipulator or carousel. It also includes ports for the following: 1) Growth sources, eight separate molecular beam oven positions equally spaced in an array opposite the sample holder, such that the nozzle of each molecular beam source is brought to focus on the substrate holder; 2) Auger analyzer and electron gun; 3) Depth profiling ion gun; 4)

Substrate cleaning gun; 5) UTI quadrapole mass spectrometer; 6) Several viewports; and 7) various other feed-throughs for pressure measurements etc. See Figure 3-1.

The entire system, including the load lock, can be rough pumped to less than ten (10) microns of mercury by three cryogenically-cooled molecular sieve adsorption.pumps. The load lock can also be rough pumped separately by one or more of these pumps. The use of adsorption pumps for this task eliminates any possible contamination of the system by oils and organic lubricants used in mechanical pumps. These molecular sieve pumps can be renewed by bakeout and by replacement of the molecular sieve beads inside the pumps.

The main pumping module lies in a cabinet below the growth chamber and contains a titanium ball sublimation pump (2000 liters/sec) surrounded by a water-cooled shroud. It is ported to a triode VacIon pump rated at 400 liters/sec for nitrogen and 84 liters/sec for argon. This pump is independently valved for isolation during conditions when the main chambers are at pressures that may be damaging to the VacIon pump. The main VacIon and sublimation pumps are also augmented by a large liquid nitrogen (LN$_2$) cryogenic pump, located above the sublimation pump, which has a pumping rate of 4000 liters/sec. These pumps serve to hold down system pressure during MBE deposition.

A second smaller VacIon pump is located in the lock between two, eight-inch viton-sealed swing valves to aid rapid pump-down of the load lock area after introducing or removing a sample at the load lock hatch.

Both the primary or growth chamber and the main pumping module, together with the load lock and all associated valves and equipment can be baked to 250°C for degassing. This helps to lower the background
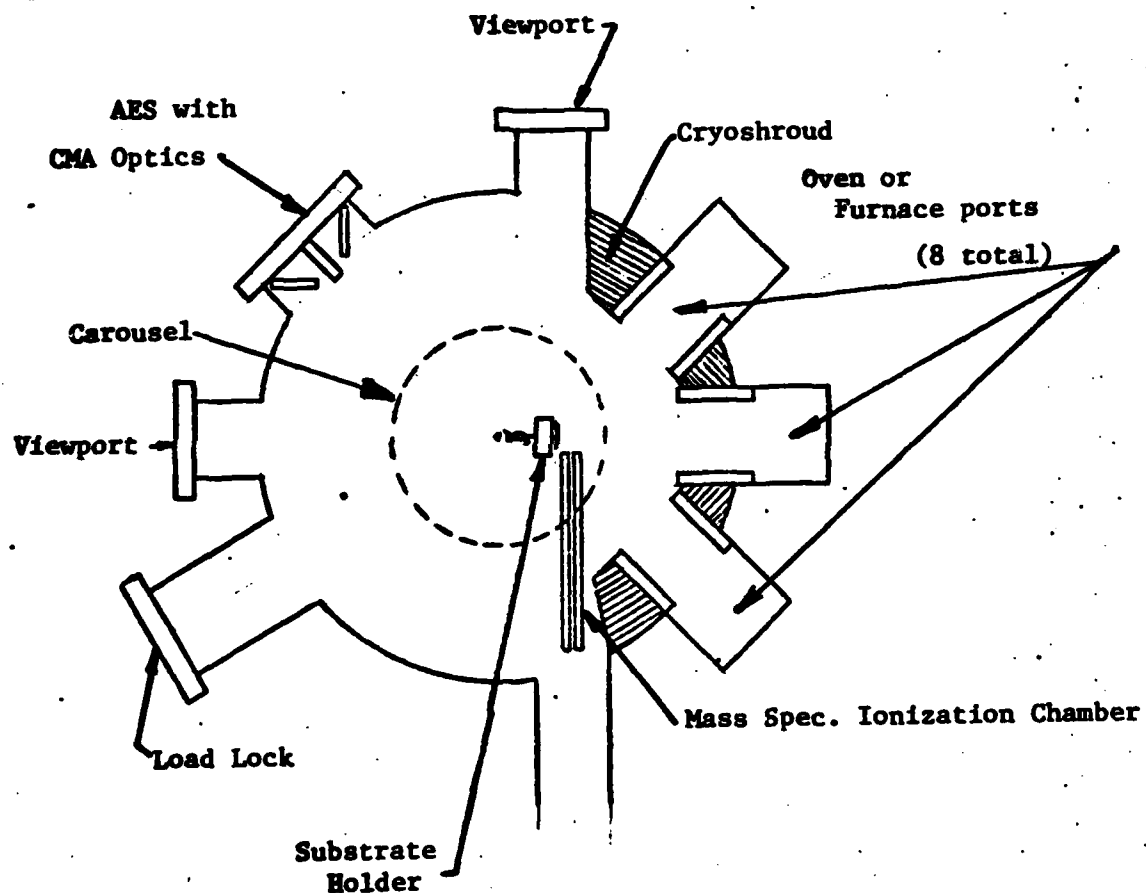
MBE System Topview

Figure 3-1 Varian 360 MBE System

26

contamination in the system. During bake-out, clamshell bake shrouds are placed over the primary chamber and the load lock. Heating is provided by non-magnetic strip heaters, mounted on the interior walls of the clamshell bake shrouds and controlled by Fenwall bi-metal switches.

Vacuum instrumentation and control are provided by multiple VacIon pump control units, a Ti-ball control unit and timer, three (one with a dual filament) ion gauges with control units, and a thermocouple pressure gauge. These controls together with the bakeout control unit are mounted on an equipment rack in proximity with the MBE vacuum system controls.

Source Configuration. Source charges of high purity arsenic (99.9999% pure), gallium (99.99999% pure), aluminum (for growing AlGaAs) and silicon (for doping) are placed in pyrolytic boron nitrate (PBN) crucibles inside the Knudsen-cell cylindrical tantalum ovens at the eight ports of the source flange. See Figure 3-2. The source flange includes source shutters for precise on and off control of the source beam and a cooling shroud for LN_2 cooling of each source position. Thermocouples attached to each oven act in conjunction with the oven's power input terminals to maintain a preset temperature (±1°C) chosen by the operator and dialed in at the Eurotherm heater control units mounted on the equipment rack. Control of the crucible temperature to within ±1 degree maintains a given gallium flux to within two (2) percent, (Ref 24).

Substrate Handling. The substrate handling system consists of a load lock with transfer boom, sample manipulator or carousel, and sample heating control. The transfer boom, on the end of which the sample holder is mounted by means of a spring-loaded clip arrangement, moves
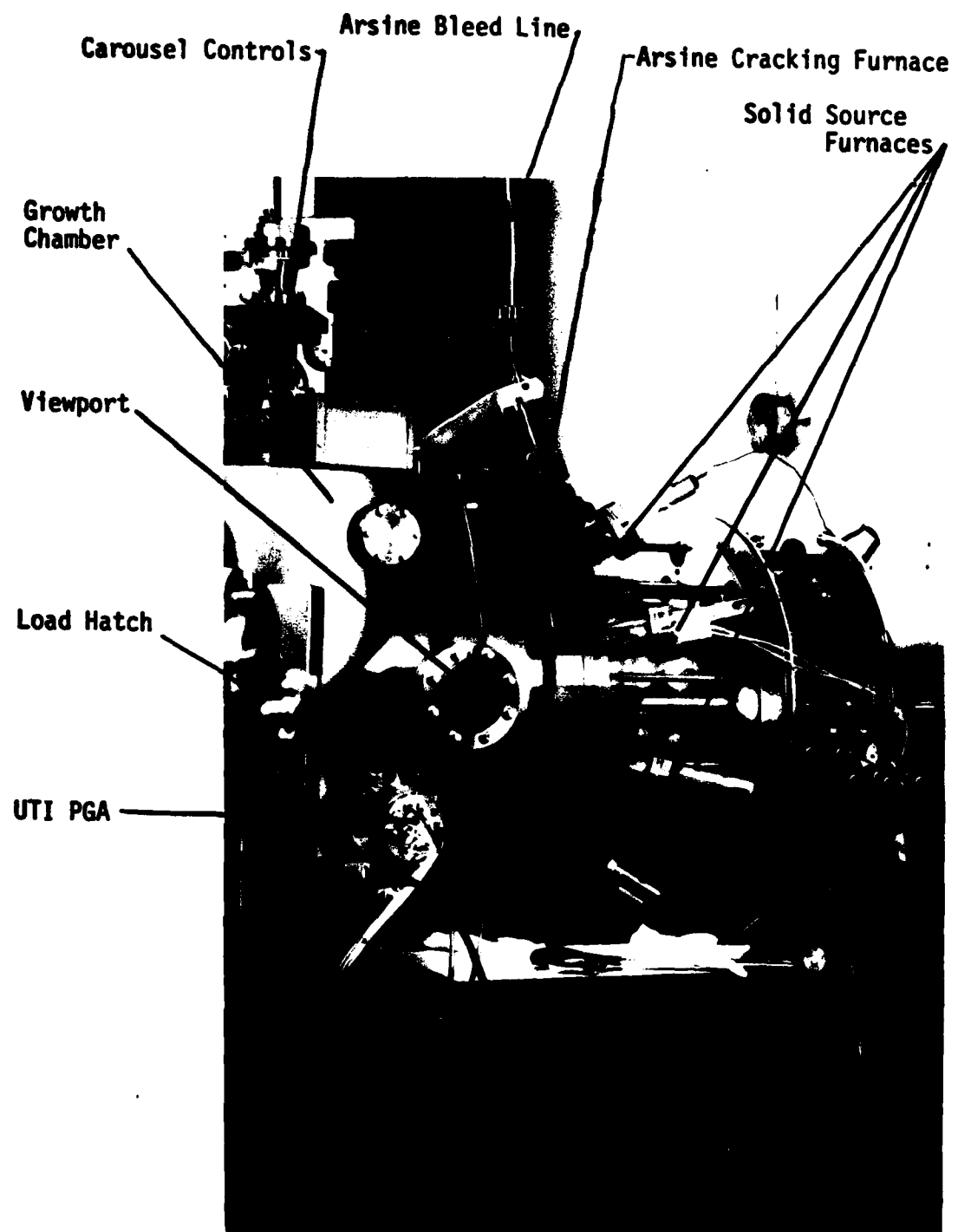
27

Figure 3-2 Photograph of Varian 360 MBE System

28

the sample from the load lock hatch to the carousel, and thus to the growth chamber of the MBE system by means of moving a long rod (transfer boom) within a long hollow stainless steel tube. This is done by sliding a magnetic sleeve, which is mounted externally on the hollow tube, toward the MBE growth chamber. The magnetic sleeve is magnetically locked to the end of the transfer boom opposite the sample holder mount. The magnetic sleeve also provides a means by which the sample is transferred to and locked into position on the sample manipulator in the growth chamber. When the sample holder is correctly positioned directly in front of the substrate heater on the carousel, rotation of the magnetic sleeve rotates the transfer boom and locks the sample holder into position on the carousel. Samples are withdrawn from the growth chamber to the load lock hatch by reversing this process.

The carousel incorporates two substrate heating positions, an ion gauge for monitoring the beam flux and a Faraday cup. It can be rotated via a bellows connection by external controls, mounted atop the growth chamber, through 360°, and can be manipulated in the x, y, and z planes. This allows for precise positioning of the sample for growth, loading and unloading, and _in situ_ analysis. The fact that the beam flux monitor is also positioned on the carousel allows for accurate measurement of the beam flux.

Epitaxy Control. In addition to measuring and controlling source and substrate temperatures, which is done using thermocouples and resistance windings, a means of controlling the molecular beam flux is needed. This is provided, primarily, by the beam flux monitor, which is mounted on the coursel on the same elevation as the substrate holder, and in addition, by a quadrupole mass specrometer, in our case a UTI

100C precision gas analyzer, (PGA). See Chapter II. The ionization chamber of the PGA is located directly below the the beam focus in the growth chamber. The PGA's control unit and oscilloscope monitor are mounted on the equipment rack and provide another means of calibrating the flux from each independently shuttered source. The mass spectrometer covers an atomic weight range from 1 to approximately 305, which makes analysis and identification of elements and polymers of high atomic weights possible. This is especially important when attempting to analyze the products of the arsine cracking furnace.

Surface Analytical Instrumentation. One of the most important aspects of experimental investigation of MBE growth is in situ analysis. This important subject is discussed in general more fully in chapter II. The configuration of the equipment used for this thesis restricted in situ analysis to Auger spectroscopy and use of the PGA.

Arsine Handling System

The construction of a system to safely handle a highly toxic gas, while not complex, required careful consideration of the following areas: 1) Arsine manifold design and construction; 2) Flow control; 3) Arsine purging and clearing; 4) Arsine monitoring and emergency procedures; and 5) Arsine cracking.

Arsine Manifold Design and Construction. In as far as possible, the arsine manifold was built as an extension of the UHV growth chamber. This choice was made to eliminate possible contaminants from entering the system and for safety reasons. Therefore the material chosen for the construction of the manifold was high purity stainless steel. Each fitting and each valve is also constructed of stainless steel. The

valves used are Nupro model SS-4H-TH3, bakeable, bellows valves with seats of different alloys of stainless steel, (these valves were welded and hermetically sealed by the manufacturer). Each joint was either welded or made by using precision machined Conflat flanges with copper gaskets. The only exceptions are the joints made at the mass flow controller and at the pressure regulator; here Swage-lok fittings join inputs and outputs to the manifold.

Before welding and assembly, each piece of tubing, each valve, each fitting, and each flange was thoroughly cleaned in hot trichloroethylene for 10-20 minutes, rinsed in acetone, rinsed in an alconox ultrasonic bath, flushed with 18 megohm deionized water, and blown dry with oil-free nitrogen. The pieces of tubing were then cut to the proper length, bent as required and again cleaned as described above. After welding and partial assembly of the manifold, each partially assembled piece was again cleaned by a trichloroethylene flush. Final cleaning was done after complete assembly by baking the entire manifold under and extended flush/purge with ultra pure hydrogen. The fully assembled arsine manifold, including the mass flow controller and the bleed line (which was temporarily welded shut at the far end) was vacuum tested to pressures less than 10^{-8} Torr.

The bulk of the arsine manifold including the flow control valve, bypass valve, vacuum roughing valve, source valves, hydrogen purge valve, arsine regulator, and the bottled arsine are contained in a secondary containment box (SCB). The SCB is constructed of ¼ inch thick plexiglass and is virtually air tight. It is vented through the ceiling and to the roof where a blower system keeps the entire apparatus under constant negative pressure (flow rate = approximately 1000 linear

31

feet/min.). To prevent possible damage to the SCB during bakeout, the portion of the arsine manifold which is inside the SCB is mounted on a ¼ inch thick asbestos-fiber board. This mounting board is in turn mounted on three, 2-inch spacers which are fastened to the rear of the SCB.

Flow Control. The arsine manifold (see Figure 3-3) not only directs the arsine from the source in the SCB to the arsine cracking furnace, but it also incorporates the means to regulate the arsine flow rate. This is done first by the pressure regulator, and again by the mass flow controller in the SCB.

The arsine regulator is a stainless steel Matheson series 3500 pressure regulator model 3501N, specifically designed to handle AsH_3 or phosphine. A Pressure regulator will maintain a constant flow rate provided downstream pressure doesn't change; a flow controller maintains constant flow regardless of downstream pressure. The electronic mass flow controller read-out is a Tylan RO-20A, 4 channel unit, where each channel has a different range. Used was channel 1, with a range of 2.00 standard liters per minute, (SLPM). The mass flow controller valve is a Model FC-260, rated at 20 standard cubic centimeters per minute, (SCCM), for hydrogen. The proper conversion factor here for arsine is .66, which corrects for the mass and thermal conductivity difference between hydrogen and arsine. So, at flow readings of 1.50 SLPM, the actual arsine flow was approximately ten (10) SCCM (Ref 25).

The third and most important means of flow control is the Varian model 951-5106 variable leak valve, which is bolted onto the cracking furnace through a Conflat flange with a copper gasket, (see Figure 3-4). The precise flow control, which is very essential to uniform crystal growth, is obtained in the leak valve by moving an optically
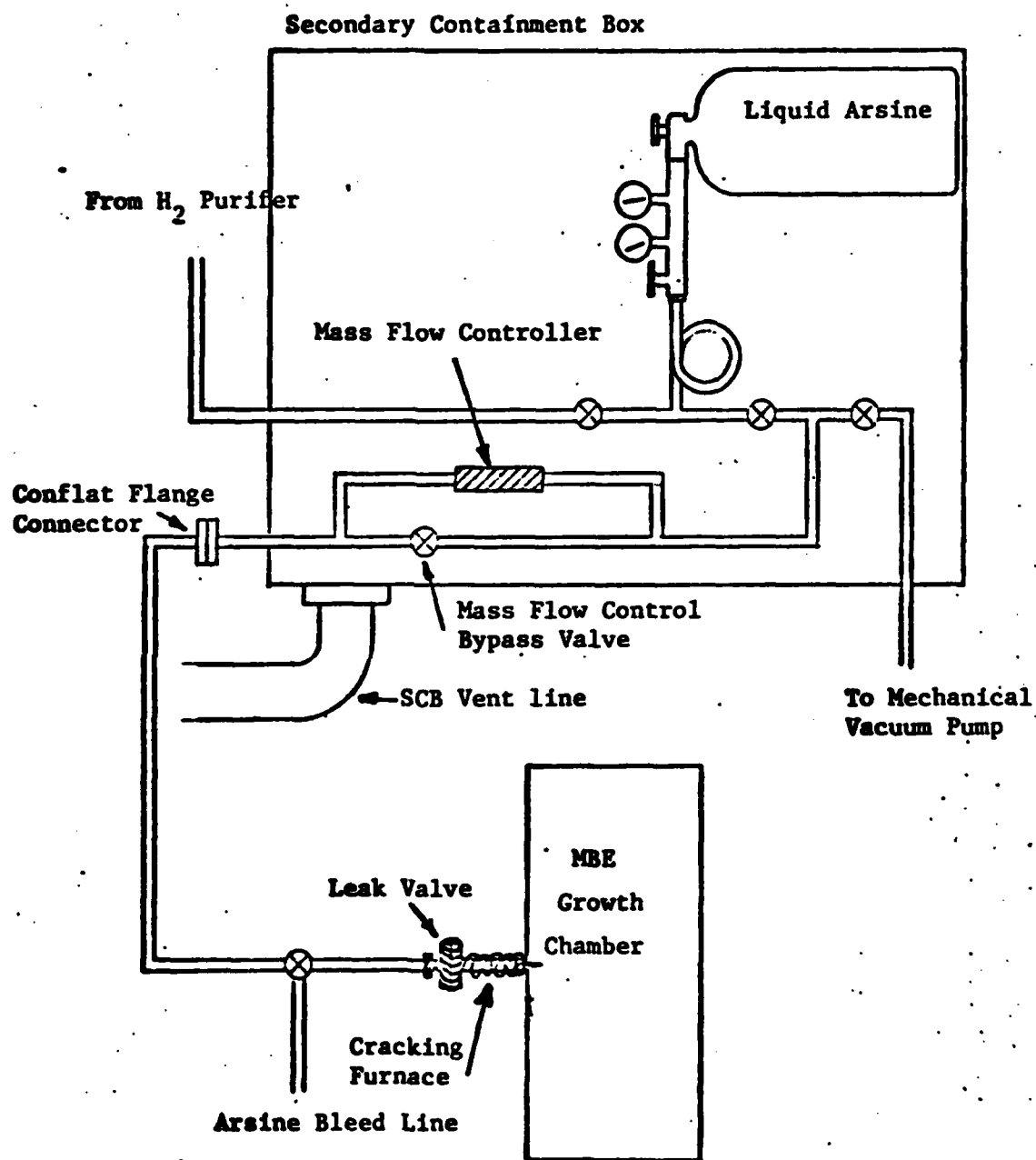
32

Figure 3-3 Arsine Manifold

Varian Model 951-5106 Leak Valve

Fine Drive Screw

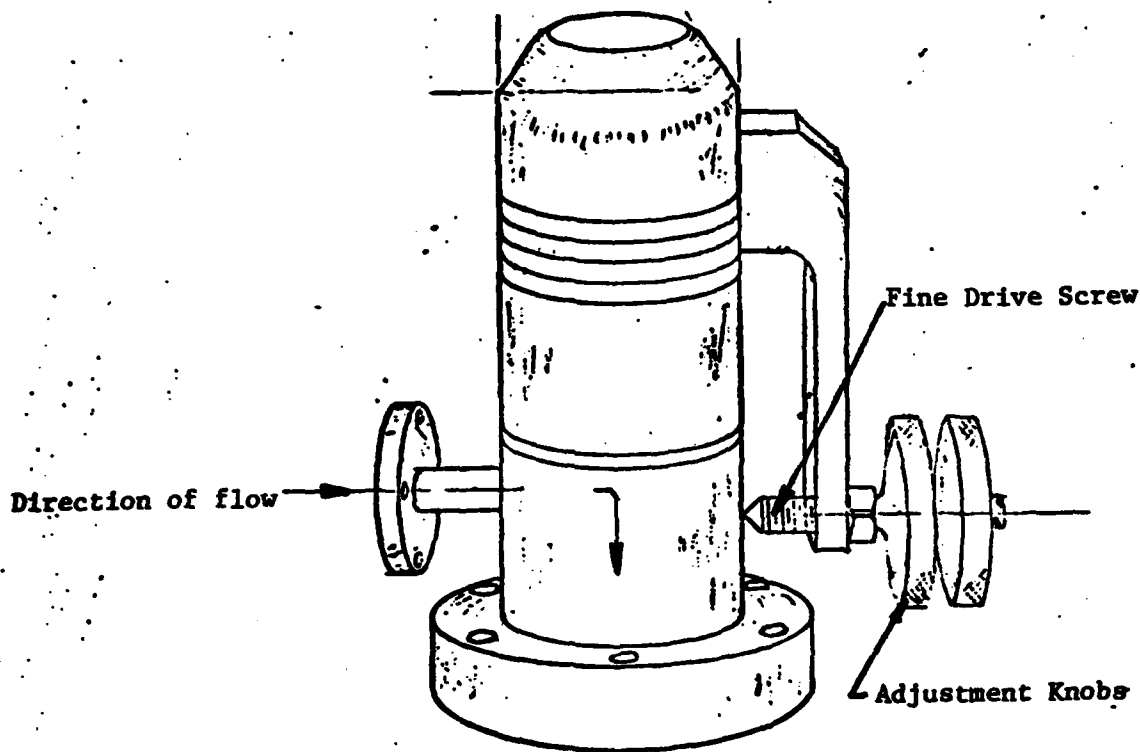Direction of flow

Adjustment Knobs

Figure 3-4 Variable Leak Valve

flat sapphire plug relative to its gold seat. Precise pressure control is achieved by observing readings on the vacuum gauges in the system (Ref 26).

To calibrate the leak valve to a zero leak condition, helium was introduced into the arsine manifold while scanning the spectrum for helium with the UTI precision gas analyzer (PGA). The knobs of the fine drive screw on the variable leak valve were set and locked at the position where helium was no longer detected by the PGA.

Arsine Purging and Clearing. To insure that the arsine manifold is not subjected to atmospheric contaminants backstreaming through the bleed line after shut down, and to rid the manifold of unused arsine trapped in the line at the end of a growth run, the manifold is purged with high purity hydrogen. At the conclusion of a run, the leak valve is closed and compressed hydrogen passes through a Matheson, model 8361, palladium diffusion cell type hydrogen purifier and into the arsine manifold through the hydrogen purge line and valve. After the entire arsine manifold and bleed line have been purged, the bleed valve and the purge valves are closed. This high purity hydrogen is then pumped from the manifold by a mechanical vacuum pump. To prevent oil contaminants from backstreaming from the mechanical pump into the arsine manifold, a liquid nitrogen cold trap is plumbed into the system between the arsine manifold and the pump. The pump is also vented to the roof. This insures that in the remote possibility that arsine should find its way into the mechanical pump, it will not be vented in the work area. The mechanical pump is used to pump the hydrogen from the manifold in preference to the main VacIon pump of the MBE system, because ion pumps do not pump hydrogen efficiently or quickly.

Arsine Monitoring and Emergency Procedures. A Matheson model 8040
arsine/phosphine monitor is installed in the system to detect any
presence of arsine in the room or inside the SCB. A three-way valve,
mounted on the SCB, is connected to the monitor's gas inlet and filter.
This valve is then used to sample air inside the SCB or room air.
Extensions on the valve facilitate the use of rubber tubing of any
desired length to sample air from anywhere in the room or SCB, and
around each joint and section of the arsine manifold.

The arsine monitor was calibrated using a model 8041 calibrator
prior to use. This required measuring the monitor's response time to
known concentrations of arsine. For each of four known concentrations,
three response times were recorded and averaged. These average times
were then compared against expected response times as given by the
manufacturer. See Appendix C. For safety, the arsine monitor was set
to detect a minimum of 0.3 parts/million AsH_3 in approximately 200
seconds.

Detailed emergency procedures for the use of arsine were developed
and practiced before the arsine was actually connected to the system.
These procedures include safety measures for the routine turn-on and
turn-off of the arsine supply, as well as procedures for handling
emergency situations such as an arsine alarm. Both routine and emergen-
cy procedures require the extensive use of Scott-Air-Pak portable
breathing units, (PBU's). See Appendix D.

Arsine Cracking. After passing through the variable leak valve,
arsine flows through another Conflat joint and then through a stainless
steel feedport welded between the Conflat joint and a ring flange, which
is in turn, mated to a conventional Knudsen-cell oven flange. Welded to

36

the feedport on the inside is a ¼ inch stainless steel bellows which makes a right angle at the center axis of the ring flange and is ceramically-sealed to a pyrex extension approximately two inches long. The small stainless steel bellows, its ceramic seal and pyrex extension, called flexible glass-end tubing, are commercially available under the brand name Cajon, model G321-4-GX-2.

The end of the pyrex glass tubing is then joined by a graded seal to a high-purity, spectrosil quartz cracking chamber, which is fitted down the center of the cylindrical tantalum heating elements of a modified Varian MBE source furnace. Two different cracking chambers were constructed. The first chamber to be used was a bulbous 3/4 inch diameter quartz tube with tapered ends. See Figure 3-5a. Three equally spaced quartz baffle plates inside the tube insure more complete cracking of the gas by increasing the mean time each molecule spends in the cracking chamber. The second cracking chamber to be designed was a 20" long, 3/16 inch diameter high-quality, spectrosil quartz tube wound into a helix so that its total length matched the total length of the hot zone in the tantalum furnace (approximately 6.5 inches). See Figure 3-5b.

Modification of the Varian MBE source furnace required removal of the following items, (see Figures 3-6 & 3-7): 1) the furnace thermocouple, 2) the tantalum disc of the furnace thermocouple assembly, 3) the crucible, 4) the furnace's rear heat shield, and 6) the center thermocouple support column, (not shown in Figure 3-7). The molybdenum standoffs and power feedthroughs were extended by 0.75 inches (this was the length added by the ring flange) using the molybdenum standoffs from a used arsenic furnace as source material. The thermocouples were

37
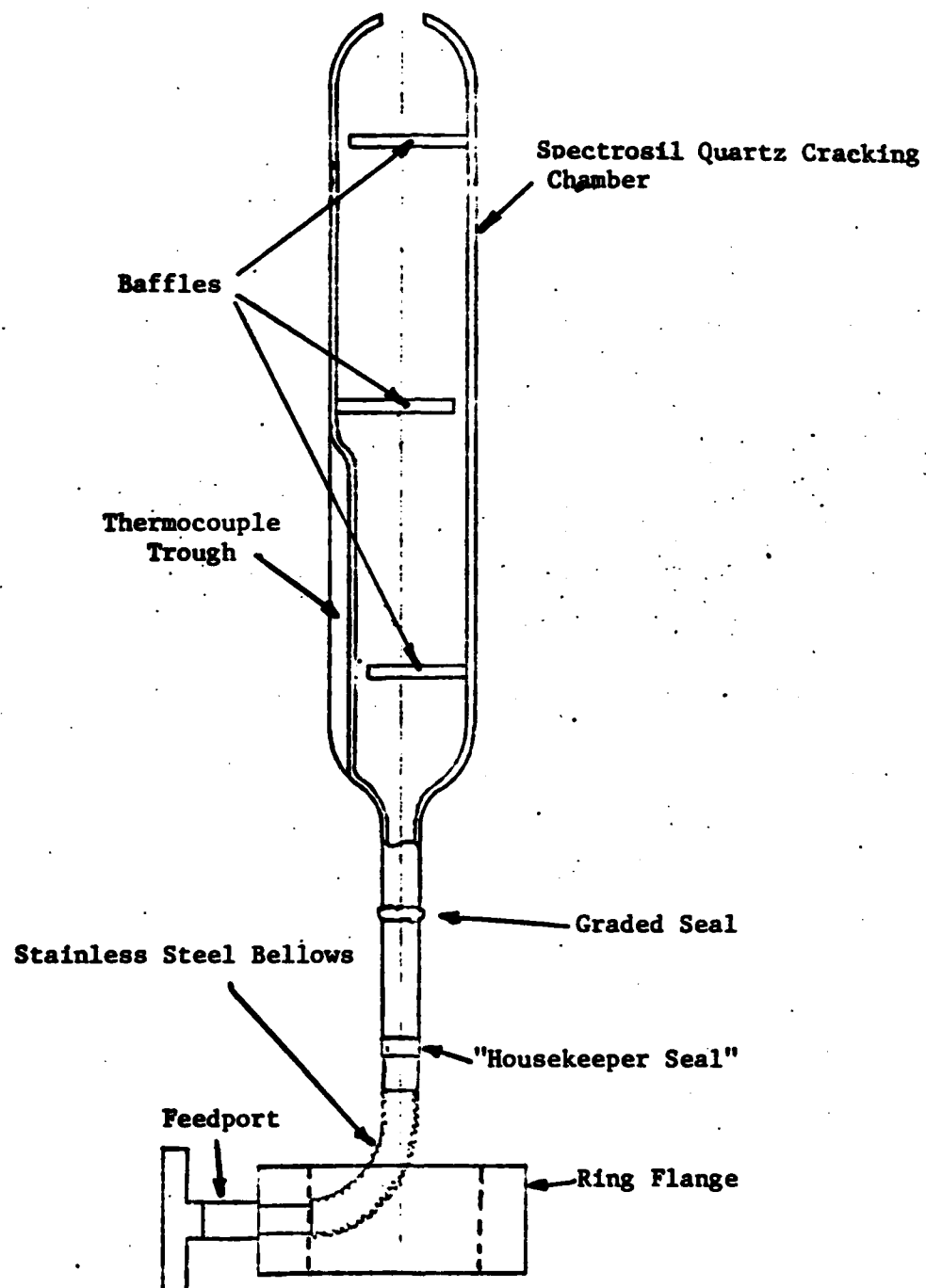
Figure 3-5a Arsine Cracking Furnace (Bulbous)

38

Cracking Chamber → ← Spectrosil Quartz

Graded Seal ——————→

"Housekeeper Seal" ——————→
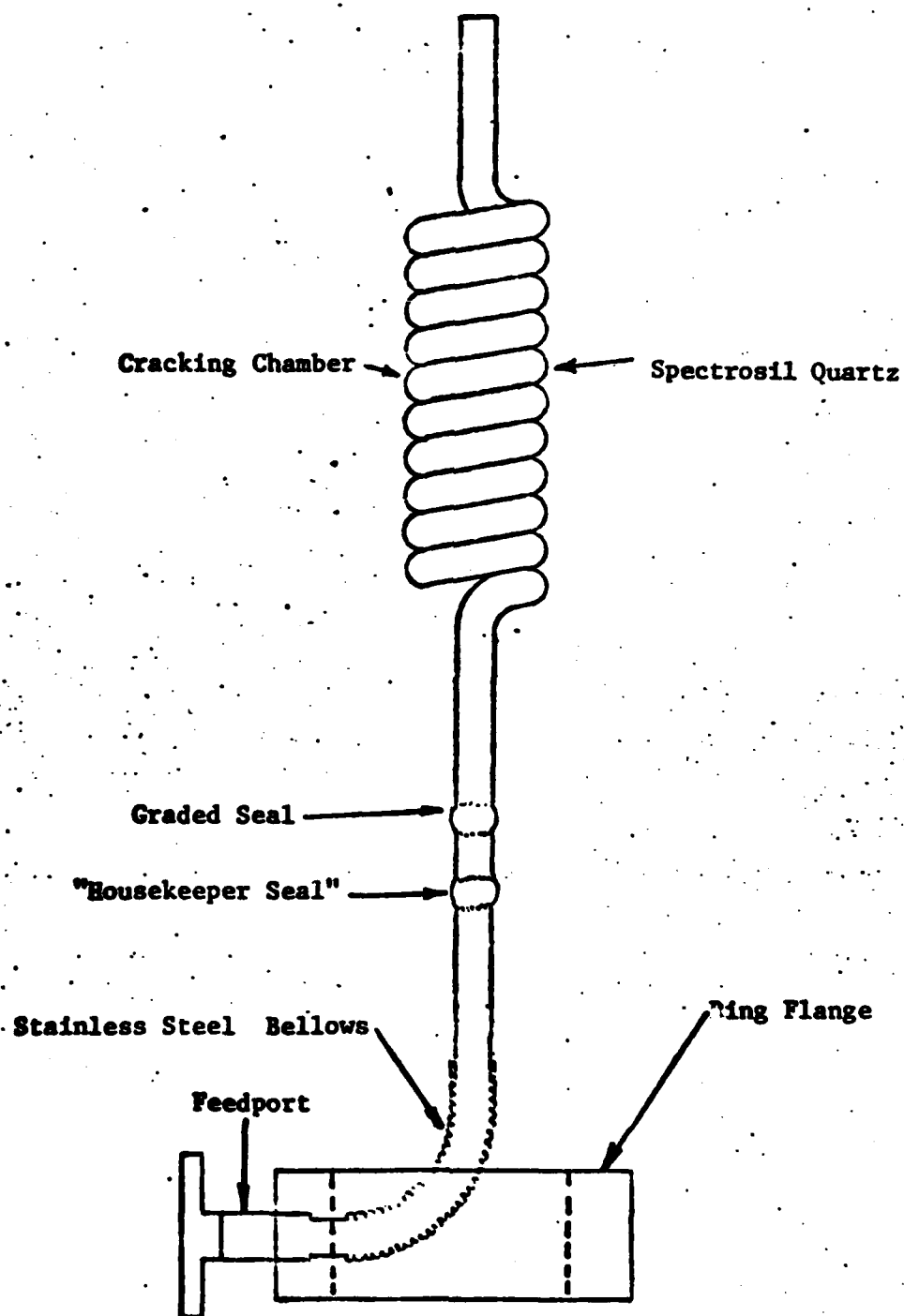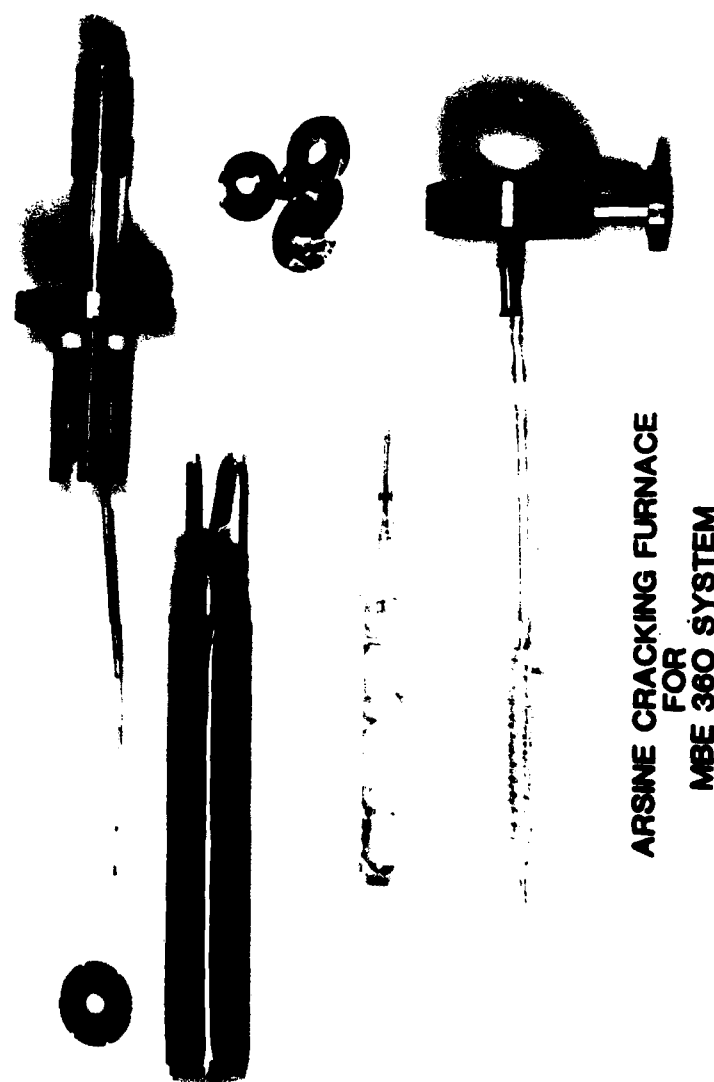
Stainless Steel Bellows

Ring Flange

Feedport

Figure 3-5b Arsine Cracking Furnace (Helical)

ARSINE CRACKING FURNACE
FOR
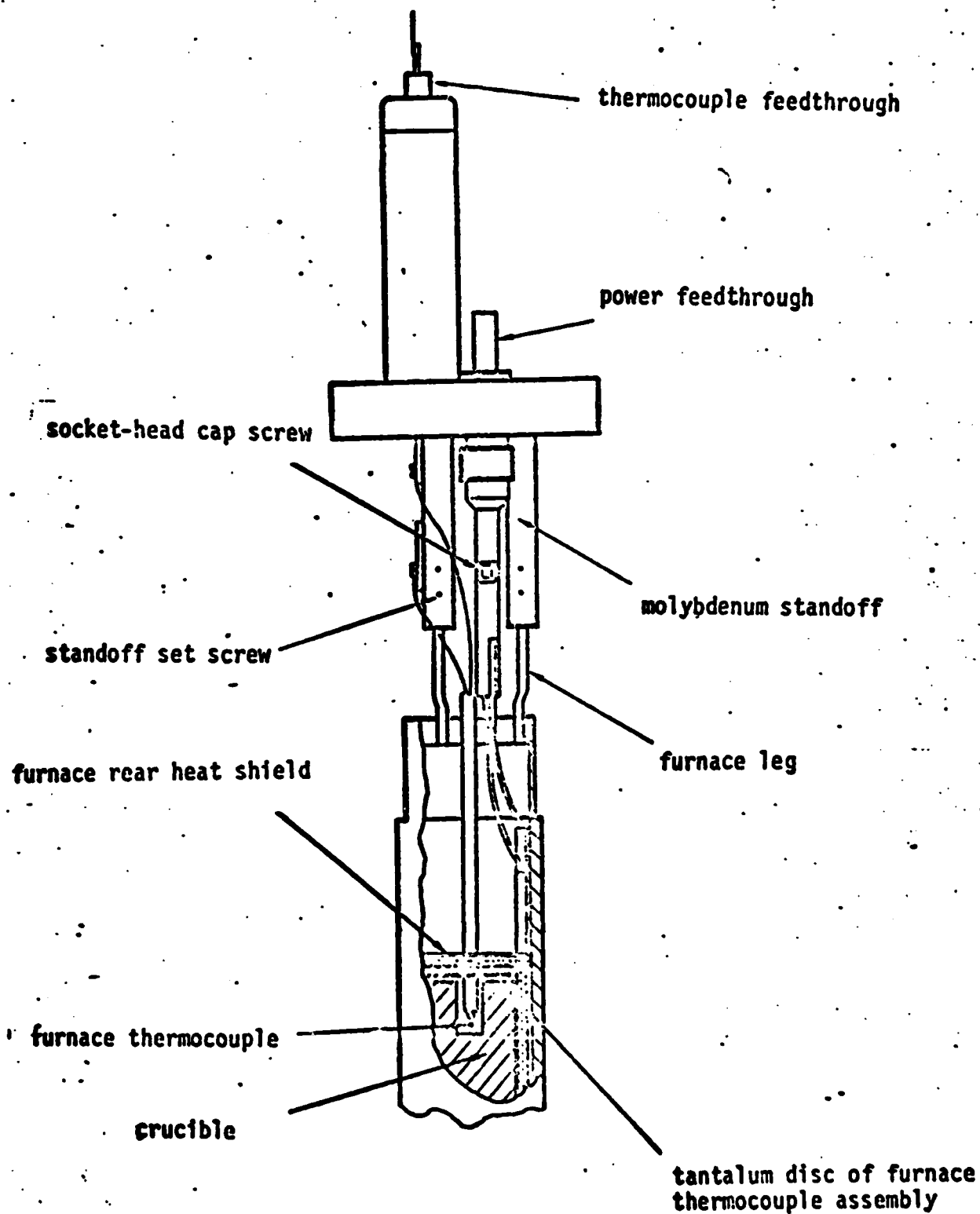MBE 360 SYSTEM

Figure 3-6 Photograph of Cracking Furnaces

Figure 3-7 Knudsen Cell Oven (Solid Source)

replaced by re-designed tungsten rhenium (W/26% Re, W/5% Re) thermo-couples, extending down to mid-length of the cracking furnace. In the case of the bulbous cracking chamber the thermocouple was placed in a shallow trough made in the chamber between the cracking chamber and the tantalum furnace. In the second case, the thermocouple was fitted in a small quartz tube fastened onto the inside wall of the helix. To prevent possible crystal contamination from the tungsten or rhenium, the thermocouple tube was closed off at the far end.

Careful assembly of the AsH$_3$ cracking furnace, allowed replace-ment of the rear heat shields (after their centers were removed). This was not done in the first design and may have contributed to the devitrifi-cation of the graded seal and eventual failure of the cracking furnace.

Although it is clear that neither cracking chamber closely approxi-mates a true Knudsen cell, (a condition which is not required), in each case a careful design of the effusing end of the cracking furnace allowed for a concentrated, well directed beam, focused at the sub-strate. The bulbous furnace was built with a circular effusing end, similar to a crucible. The helical furnace ends in a one-and-one-half inch long straight section of quartz tubing, located at the axial center of the furnace, and extending through a front heat shield at the front of the furnace.

IV. PROCEDURES AND RESULTS

Procedures

Substrate Preparation. One of the most important aspects of
quality semiconductor growth is the proper cleaning and handling of the
crystal substrate, this is particularly true for MBE growth. This is
true because MBE lacks the convenient in situ etch-back of other tech-
niques (LPE and VPE) which can uniformly remove surface impurities (1-3
microns) due to handling.

Although ion sputtering was used extensively in early MBE work for
substrate cleaning inside the UHV chamber, it has largely been abandoned
in more recent work due to the great number of unknowns about its
possible side effects, most notably, the surface damage it causes. More
work needs to be done in this area.

The substrates used in this work were all commercially-prepared,
chromium-doped GaAs crystals, whose [100] faces were cut and polished
before receipt in the laboratory. Each sample was carefully cleaned in
a bath of hot/cold trichloroethylene (10 minutes-hot, 10 minutes-cold)
and rinsed thoroughly with acetone and 18 megohm deionized water before
etching. Pre-etch cleaning then included a 10 minute ultra-sonic bath
in alconox, and again a thorough flush with deionized water. With the
substrate sample still wet from flushing, it was carefully immersed,
face-side up, in a cold solution of 3-parts sulfuric acid, 1-part
deionized water, and 1-part hydrogen peroxide. This was followed by yet
another flush with d.i. water and a thorough blow-drying using contami-
nant-free helium.

43

Normally, as soon as a sample was cleaned, it was transferred to the clean area for mounting on the substrate holder; two exceptions were samples 194 and 195, which were first "buffered" with a 3-micron thick layer of GaAs deposited by means of VPE. The mounting of the sample was done by carefully wetting the back of the sample with melted indium (99.999% pure) and placing it carefully and firmly on the polished molybdenum substrate holder (which had been previously cleaned in the manner described above without the etch). The indium insures uniform heating of the sample and keeps it firmly in position by surface tension adhesion. The sample was also fastened in the 6 o'clock position by a ledge, which extended slightly over the edge of the sample. The ledge was screwed into place using a molybdenum screw, which also held a growth-step indicator, which shadowed a small area of the sample during deposition and provided an accurate means of determining the thickness of the growth. The ledge, the screw, and the growth-step indicator had all been cleaned as described above.

Prior to mounting the sample on the transfer boom as described in chapter III, it is necessary to "vent" the load lock area with dried argon; this minimizes possible contamination of the load-lock. When the sample has been mounted on the transfer boom, and the load-lock area has been pumped down to near UHV conditions, the sample is then transferred to the carousel.

Establishing the Parameters for Growth. Before any surface deposition could begin it was obligatory to calibrate the arsine cracking furnace. This proved to be a difficult, time-consuming task. First, under conditions approximating expected optimum growth, careful measurements of flux and chamber vacuum were noted. Then, using the PGA,

comparative readings for As_1, AsH_1, AsH_2, and uncracked AsH_3 were recorded. This was done both before establishing a flow of arsine through the furnace and after. Vacuum conditions were set at approximately 1×10^{-9} Torr, background, and slightly lower (4.0×10^{-9}) for an arsine flow rate of 10 SCCM, (See chapter III). The leak valve was set approximately two turns from fully closed. Next, keeping the above parameters constant, the temperature of the AsH_3 cracking furnace was increased over the range 300°-1000°C. The percentages of each cracked constituent are are plotted in Figure 4-1a. Figure 4-1b shows the relationship between the partial pressures and temperature. Figures 4-2 and 4-3 show a comparison between the PGA oscilloscope traces for cracked and uncracked arsine respectively, for the bulbous cracking furnace first constructed.

The helix furnace proved more difficult. For, while the two furnaces behaved in a very similar manner at low mass flow rates through the leak valve, at high rates of flow, the cracking ceased entirely, or at least was no longer perceptible under the restrictions of accuracy placed on us by the mass spectrometer, (See Chapter II). This problem was likely to have been present in the bulbous furnace as well, but was not investigated due to devitrification of the furnace's graded-seal and its subsequent replacement.

Results

Samples 193, 194 and 195. Using the bulbous cracking furnace, and based on Calawa's results (Ref 6) and the preliminary, at times, seemingly-inconsistent results we were able to achieve,-- MBE sample 193 was grown on a prepared Materials Research Center substrate, oriented 3°
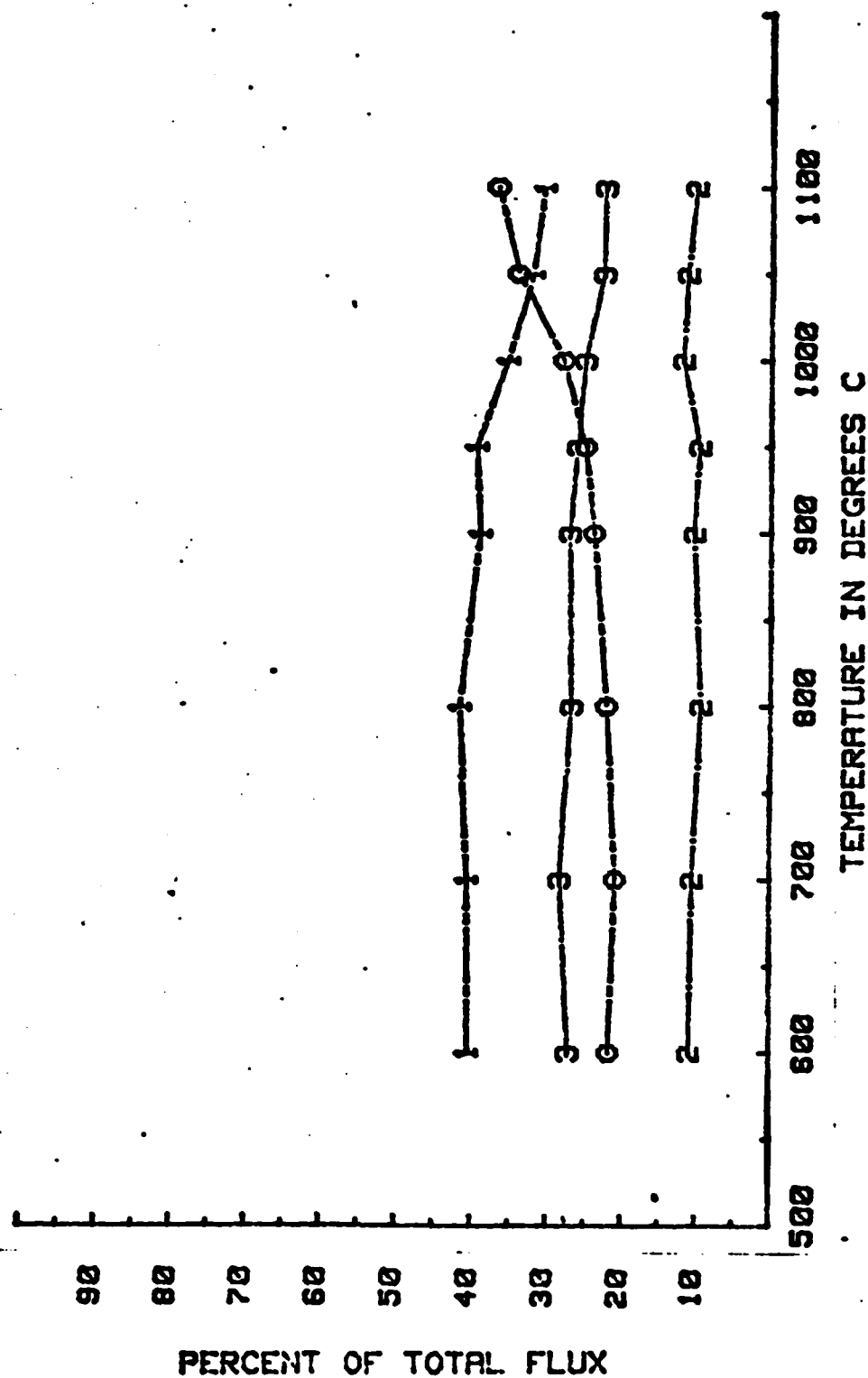
Figure 4-1a Plot of Arsine Cracking (percent) vs. Temperature

46

Figure 4-1b Plot of Arsine Cracking (pressure) vs. Temperature

47

Temperature 550 C

AsH$_1$

AsH$_2$

AsH$_3$

As
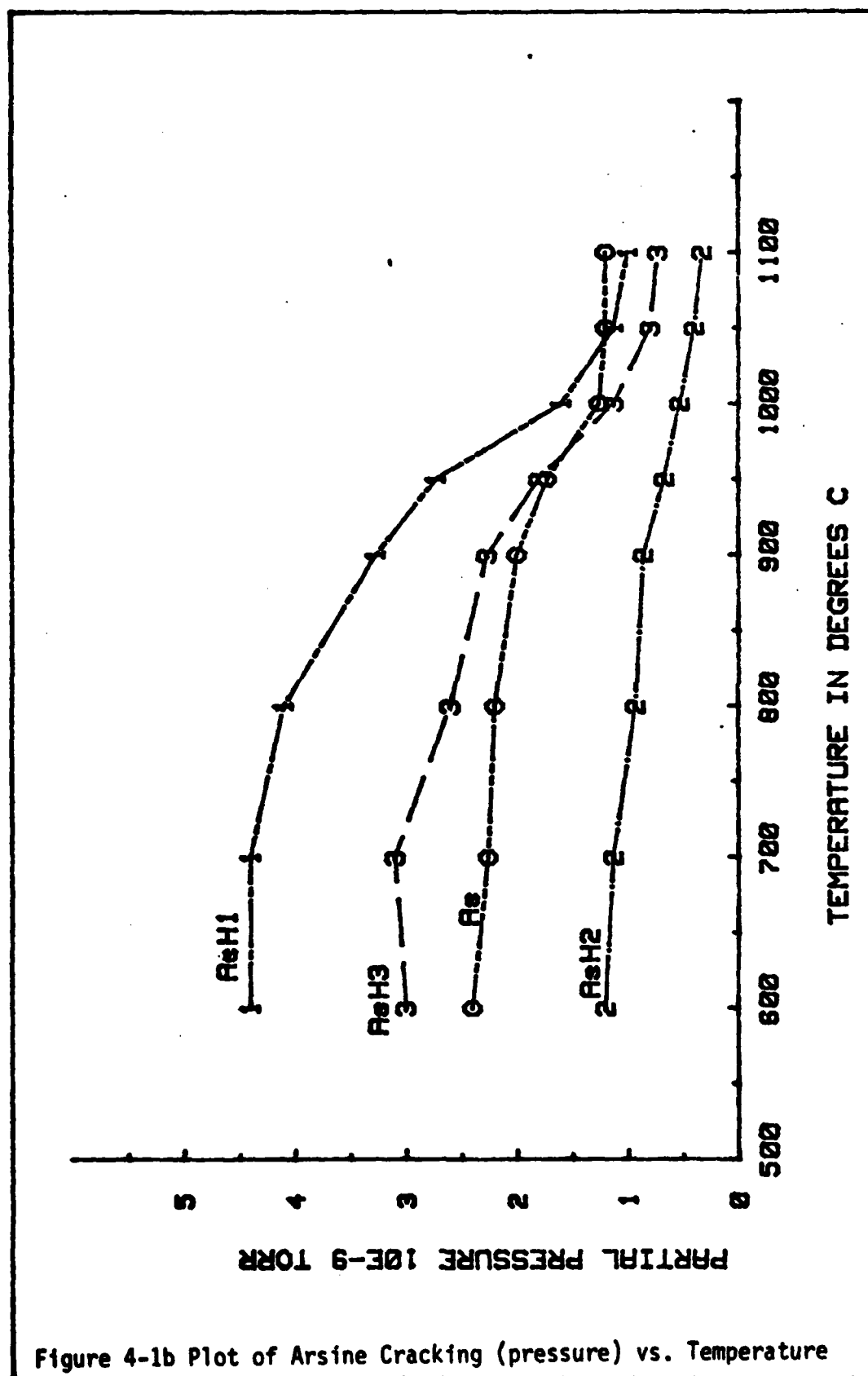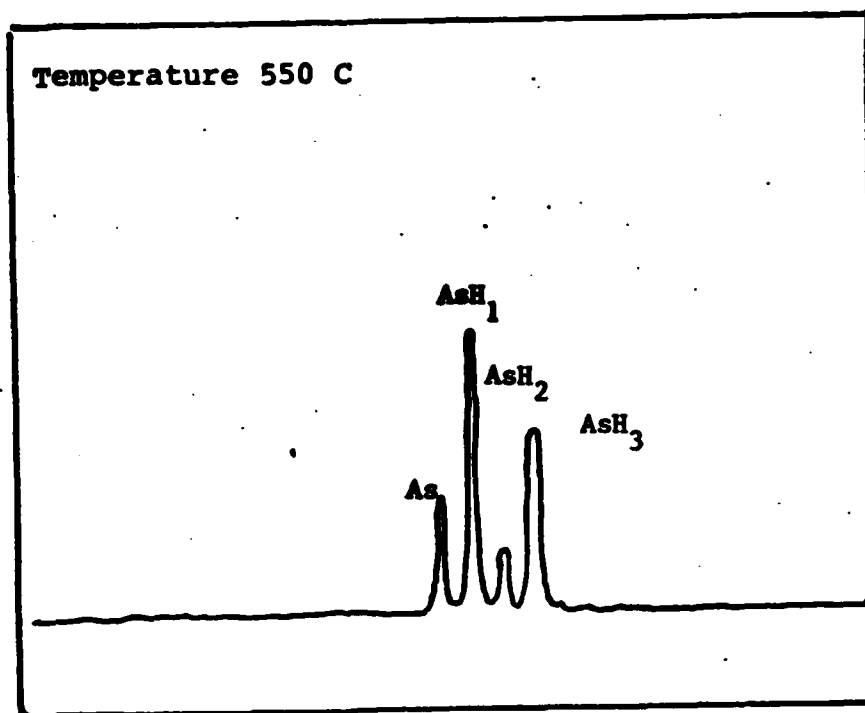
Figure 4-2 Oscilloscope Trace of Uncracked Arsine

Temperature 850 C
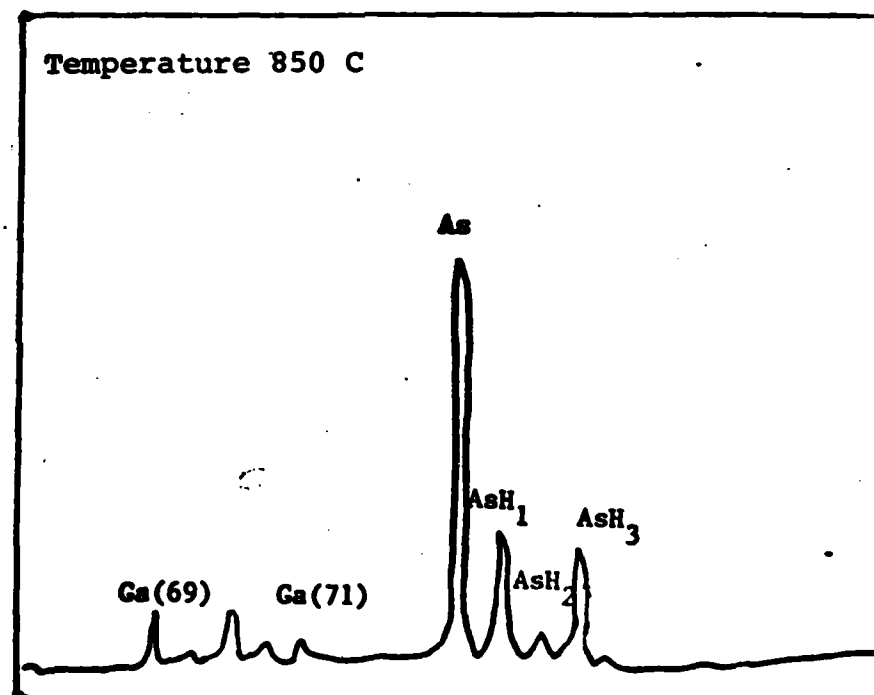
As

AsH$_1$

AsH$_3$

AsH$_2$

Ga(69)

Ga(71)

Figure 4-3 Oscilloscope Trace of Cracked Arsine

from [100] toward [110]. The gallium oven was set at 1000°C, the arsine cracking furnace at 1050°C, and the substrate temperature at 650°C. The usual precaution of keeping a constant stream of arsenic focused on the substrate at temperatures above 400°C was followed. Background beam fluxes for Ga and As were 1.8×10^{-9} and 2.5×10^{-7} respectively. Shutter-open fluxes were 1.65×10^{-7} for Ga and 4.0×10^{-7} for As. The growth run was for 6 hrs. Figure 4-4 is a microphotograph of the sample's edge under 800 power magnification, which shows the growth on this area of the sample to be approximately 5 microns. The growth was not uniform over the surface of the sample however. Figure 4-5 is a composition microphotograph of the sample en-face at a magnification of 800 in growth and non-growth areas respectively. The large droplets visible on the surface are probably gallium droplets, since gallium is liquid at near room temperatures. The growth is obviously polycrystalline.

An Auger analysis of the surface of sample 193 (Figure 4-6) showed the surface to be arsenic rich, a result which has not yet been brought into full consonance with other tests run on the sample, but is probably due the polycrystalline morphology of the surface. Table III summarizes the results of the sample's Hall-Effect measurements. For comparison, Table IV is a summary of the Hall measurements of sample 192 which was grown using a solid source of arsenic. C-V profiling could not be done because the sample was not sufficiently monocrystalline to allow analysis using the laboratory's equipment. The photoluminescent studies made of the sample were not very illuminating (no pun intended), showing only a broad, non-resolved spectral band, confirming the polycrystalline nature of the sample.
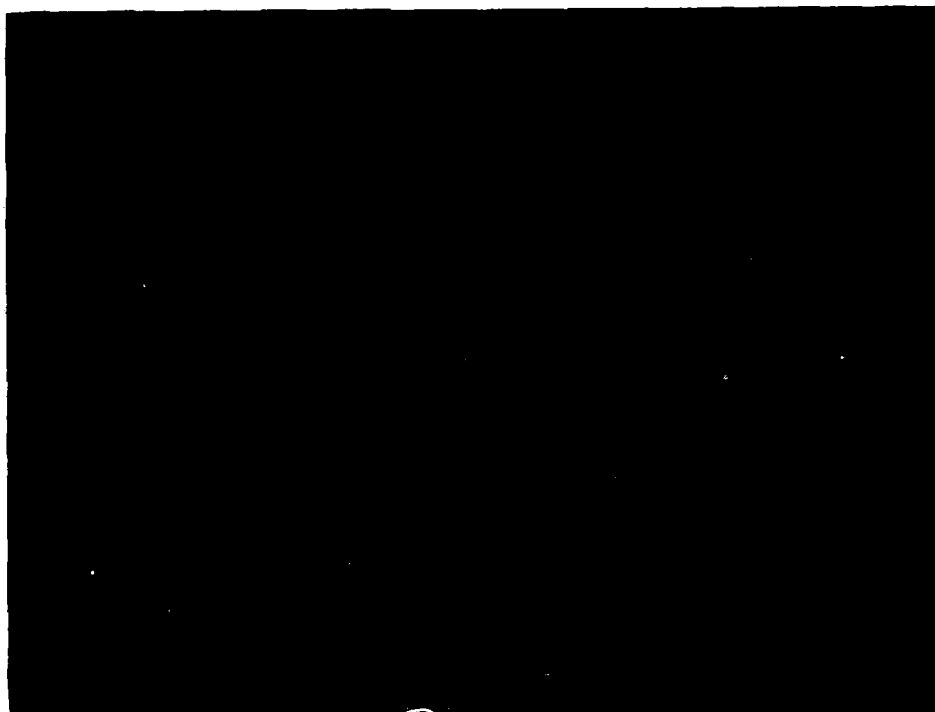
Figure 4-4 Microphotograph of Sample 193 in Profile

Growth Area   Non-growth Area

Figure 4-5 Composition Microphotograph of Sample 193
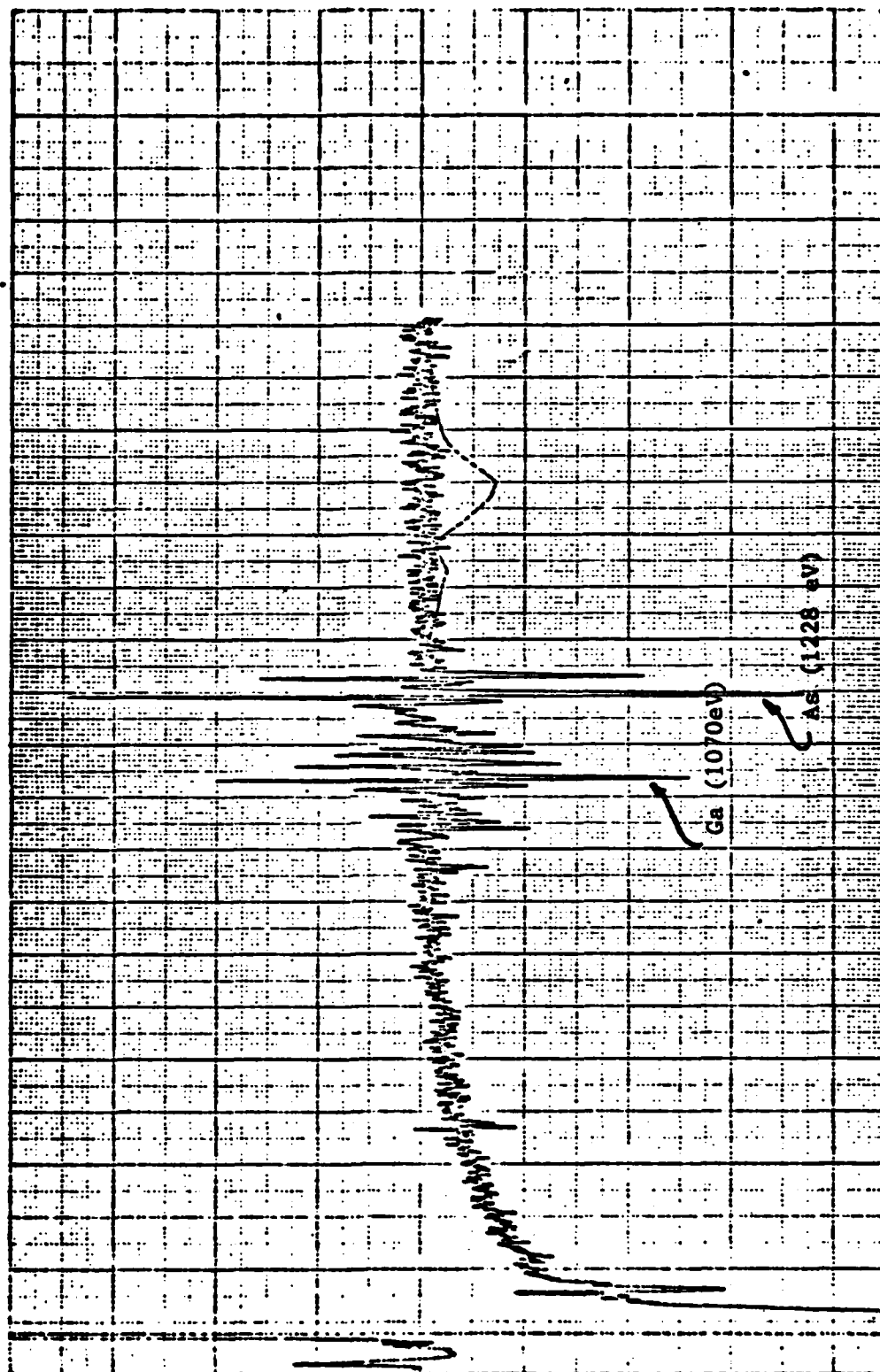
Figure 4-6 Auger Analysis of Sample 193 (Beam Energy 9KeV)

51

Table III

Summary of Hall Measurements for Sample 193

I (amps)	B (Gauss)	TYPE	RHO (Ohm-cm)	MU (cm^2/v-sec)	CONC (cm^{-3})
4.760E-09	-4494	P	1.036E+04	5.251E+00	1.149E+14
-4.640E-09	-4492	N	1.087E+04	4.655E+00	1.236E+14
4.760E-09	4501	P	1.057E+04	3.389E+01	1.745E+13
-4.620E-09	4501	P	1.078E+04	2.880E+01	2.013E+13
Averaged Over Current and Magnetic Field					
			1.064E+04	1.817E+01	6.902E+13

Sample: MBE-Ga193L, Temperature: 296K, Thickness: 1 Micron

52

Table IV

Summary of Hall Measurements for Sample 192

Sample: MBE-Ga192, Temperature: 77K, Thickness: 7 Microns (7.6 Microns)

I (amps)	B (Gauss)	TYPE	RHO (Ohm-cm)	MU (cm^2/v-sec)	CONC (cm^{-3})
6.780E-04	-4501	N	4.749E-01	4.971E+04	2.648E+14
-6.690E-04	-4501	N	4.821E-01	4.952E+04	2.618E+14
6.780E-04	4501	N	4.822E-01	5.029E+04	2.577E+14
-6.680E-04	4501	N	4.896E-01	5.023E+04	2.542E+14

Averaged Over Current and Magnetic Field

			4.822E-01	5.001E+04	2.596E+14

Temperature: 296K

| I (amps)	B (Gauss)	TYPE	RHO (Ohm-cm)	MU (cm^2/v-sec)	CONC (cm^{-3})
8.760E-05	-4506	N	3.555E+00	7.473E+03	2.352E+14
-8.720E-05	-4506	N	3.672E+00	6.338E+03	2.685E+14
8.760E-05	4498	N	3.588E+00	7.461E+03	2.334E+14
-8.710E-05	4498	N	3.685E+00	6.360E+03	2.667E+14

Averaged Over Current and Magnetic Field

			3.625E+00	6.891E+03	2.510E+14

Calculated Values: $N_D = 1.3 \times 10^{15}$, $N_A = 1.0 \times 10^{15}$.

53

In an effort to obtain better nucleation, the following parameters were changed for sample 194: 1) The AsH_3 cracking temperature was reduced to 850°C, and 2) The substrate temperature was reduced to 580°C. In each case the change was made to increase the amount of arsenic available for nucleation.

Unfortunately, the results for sample 194 showed much the same polycrystalline morphology evident in sample 193. If any progress had been made, it was in the uniformity of the growth pattern. The entire face of the crystal had a light, milky appearance, characteristic of a gallium-rich polycrystalline surface. Extensive analysis of sample 194 proved to be of little value. It was not known at the time, but by the end of run 194, the graded seal of the cracking furnace was probably already in the advanced stages of devitrification. Several clues stirred our suspicions that the problems we were having didn't all stem from setting incorrect parameters. First, inspite of multiple degassings, the PGA seem to indicate that the rate of cracking in the furnace was decreasing, and this was happening uniformly over all temperatures. Second, the adjustments we had made in the growth parameters should have had a much more dramatic effect on the gallium to arsenic flux ratio and thus on the surface morphology than was evident.

Sample 195 was not unlike the two samples which preceded it, except in one important way. At the conclusion of the run sample 195 was viewed in white light through one the viewports. It looked polycrystalline, like the other samples, but it had a grayish hue. Our suspicions about possible oven failure were confirmed when AES analysis showed an inordinate amount of silicon on the surface. See Figure 4-7.
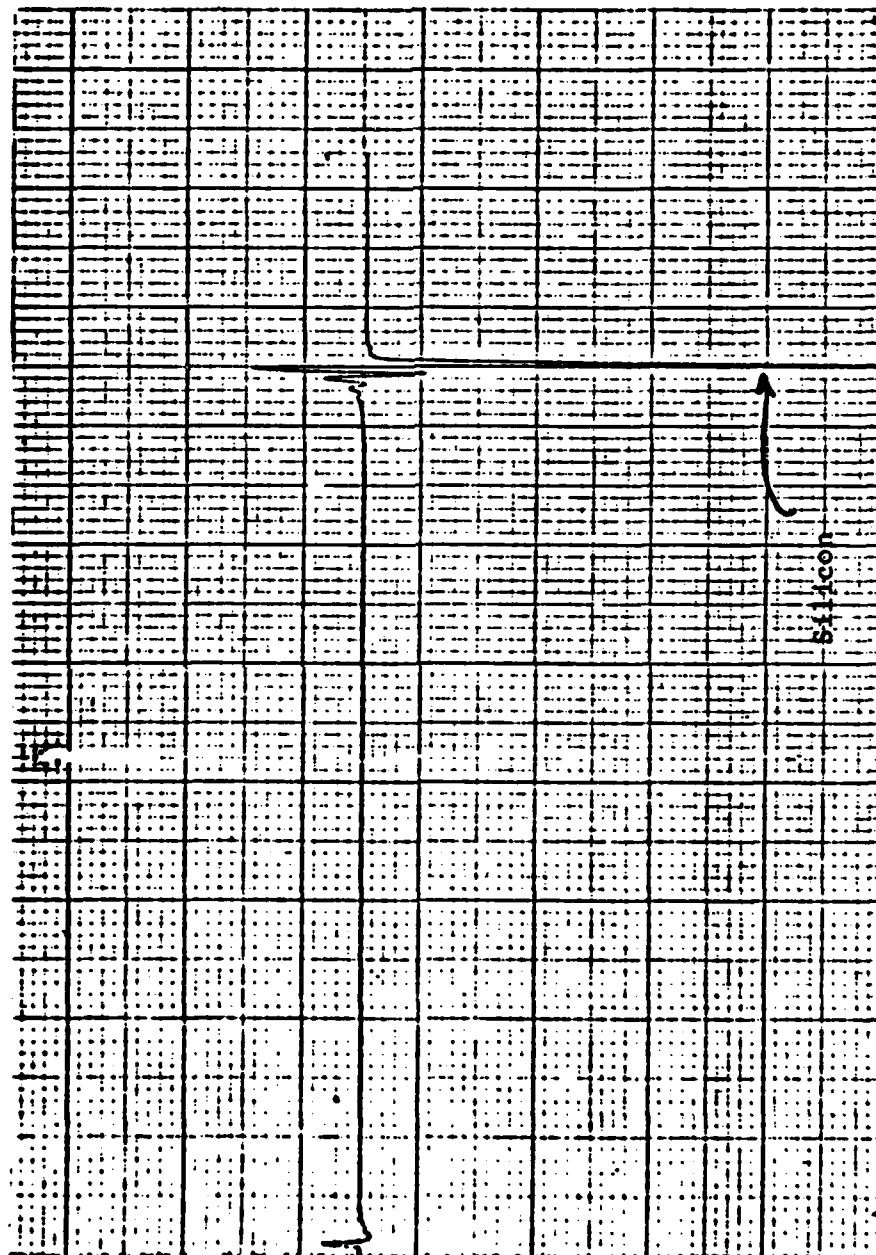
Note: At this sensitivity the AES shows nothing but Silicon.

Figure 4-7   AES of Sample 195 (Showing Silicated Surface)

Sample 196. Only one sample has been grown to-date using the helix cracking furnace. While not all of the analytical results have been received at this point, it is known that the growth is non-uniform , (possibly due to the high directionality of the design), and that it is likely to be highly polycrystalline. Further results will be added as Appendix E.

V. Conclusions and Recommendations for Further Study

Though we were not successful, as yet, in growing GaAs, or even in establishing the parameters for uniform nucleation, considerable progress has been made in marking the path for further study. Urgently needed is a better understanding of arsine cracking. Neither Calawa nor Panish (Ref 27) have provided us with enough information to firmly establish what the cracking mechanism is. Is it primarily thermal dissociation that is responsible for the cracking of arsine, or is it a catalytic, or perhaps a photolytic process? The answers are certainly not clear. The results we have achieved, with each furnace, suggest that thermal cracking alone may not provide sufficient As_1 or As_2 for quality MBE growth. A slight modification in the design of the cracking furnace to incorporate a tantalum wire down its bore would help shed light on this question. Furthermore, if the wire could be connected across one of the heating terminals and ground, it would allow the Ta wire to be heated independently of the cracking furnace.

Other improvements in design might incorporate a way to measure the drop in pressure across the leak valve. It is certainly possible that the instabilities observed in the cracking pattern of arsine at higher mass flow rates were due, in part or whole, to supersonic flow of the arsine gas through the furnace. This conclusion seems to be borne out by the highly focused growth pattern of sample 196. Professor Stevenson, et al, reported in their article (Ref 28) having observed a decrease in beam intensity as the temperature was increased in a hydrogen furnace where a gas was being leaked through a small orifice into UHV conditions. They ascribe this decrease in beam density to both a

57

decrease in gas density inside the furnace and to supersonic flow. Further, they make the claim that the maximum axial Mach number is greater than 10. Surely, if the flow rates inside our cracking furnace are even an order of magnitude smaller, then arsine molecules spend so little time in the heated area of the furnace they may not have reached their dissociation temperature. Unfortunately, this is merely speculation. What is certain is that the cracking pattern observed by the PGA was primarily a function of flow rate through the helical cracking furnace, and not a strong function of temperature. A return to a furnace design more like the first one, perhaps with more than three baffle plates, is a step that should be taken to see if this was due to cracking furnace geometry or to the cracking mechanism itself.

Another area of interest is the presence of As_2 and As_4 as products of arsine cracking. Calawa indicates in his work that the dimer and the tetramer are present in significant amounts when arsine is cracked. He speculates that recombination may be responsible for the high levels of these species. We found no trace of either As_2 or As_4 with the first cracking furnace. The second furnace did show a small trace of As_2, but only by using the very highest gain level (10^{-12}) of the PGA. Figure 5-1 is an oscilloscope trace which shows the presence the As_2 species. No trace of As_4 was ever detected. This result is surprising, and demonstrates again that the cracking mechanisms are poorly understood at present.

Perhaps a laser could be used to investigate AsH_3 cracking under UHV conditions, in a manner similar to the method described in reference 19, where a laser operating at 193 nm is used to dissociate arsine. A primary difficulty is the small molecular cross section of each species under UHV conditions.
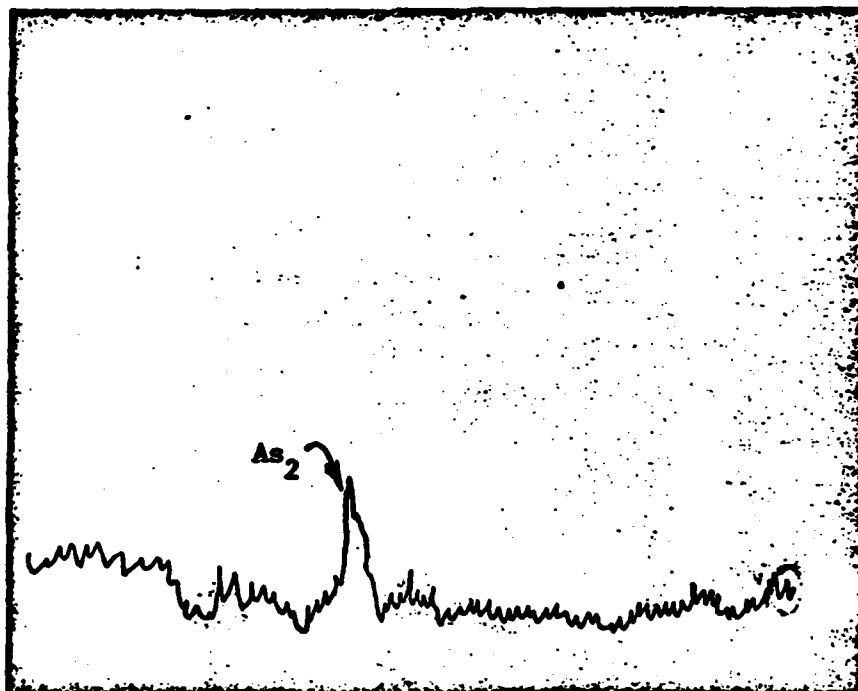
Figure 5-1 Oscilloscope Trace Showing Presence of As_2

59

Bibliography

1. K. G. Guenther, Naturwissenshaften 45(1958) 415.

2. K. G. Guenther, in "The Use of Thin Films in Physical Investigations", Ed. J.C. Anderson (Academic Press, London, 1966) p. 123.

3. B. A. Joyce and C. T. Foxon, Journal of Crystal Growth, 31(1975) 122-129, North Holland Publ. Co.

4. A. Y. Cho and J. R. Arthur, "Molecular Beam Epitaxy", Progress in Solid-State Chemistry, Vol 10, Part 3, pp.157-191, Pergamon Press 1975, Great Britain.

5. J. E. Davey and T. Pankey," Epitaxial GaAs Films Deposited by Vacuum Evaporation", J. Appl. Phys. 39, 1941(1968).

6. A. R. Calawa, Applied Physics Ltr.38 (9), 1 May 1981, pp.701-703.

7. Low, Stillman, Cho, Morkoc, & Calawa, Appl. Phys. Lett. 40, 611, (1982).

8. F. Reif, Fundamentals of Statistical and Thermal Physics, McGraw-Hill Inc. 1965 pp. 271-274.

9. J. P. McKelvey, Solid State and Semiconductor Physics, Harper and Row , N.Y., 1966 pp. 289.

10. F. Bloch, Zeitschrift fuer Physik, (1928) 52, 555.

11. R. A. Smith, SemiConductors, 2nd edition, Cambridge Univ. Press, 1978, pp 24-37.

12. A. S. Grove, The Physics and Technology of Semiconductor Devices, Wiley & Sons, Inc. 1967 pp. 102-103.

13. A. R. Calawa, 1978 Annual Report to the Air Force Office of Scientific Research, #ESD-TR-78-397, 1978. p. 3.

14. A.Y. Cho and J.R. Arthur, Progress in Solid State Chemistry, Vol 10, Part 3, p.158. Pergamon press 1975, Great Britain.

15. R. D. Burnham, D. R. Scifres, Prog. Crystal Growth Charact., Vol 2, pp.95-113.

16. S. Kishino, H. Nabashima, N. Chinone and R. Ito, Applied Phys. Letters, 31, 759(1977).

17. Davis, et al, Handbook of Auger Electron Spectroscopy, 2nd Ed. Physical Electoronics Industries Inc. Eden Prairie, MN, 1976.

Bibliography

18. D.A. Stevensen, et al, in "Control of Impurities in the Epitaxial Growth of High Quality GaAs", Technical Report #CMR-77-4, p.6.

19. V.M. Donnelly and R.F. Karlicek, in "Development of Laser Diagnostic Probes for Chemical Vapor Deposition of InP/InGaAsP Epitaxial Layers", Bell Labs, Murray Hill, NJ. (To be published in J. of Appl. Phys. 1982).

20. UTI 100C Precision Mass Analyzer, Operating and Service Manual, Appendix B, pp. 1-4.

21. A.S. Grove, The Physics and Technology of Semiconductor Devices, Wiley and Sons, Inc. 1967 pp.169-172.

22. C.W. Litton, Air Force Avionics Lab Technical Report #78850104 p. 28, 1974.

23. Varian 360 MBE System Instruction Manual, Section 3, Varian Vacuum Division, Palo Alto CA. 1978.

24. L.S. Smirnov, in "Problems of the Radiation Technology of Semiconductors", Publishing House "Nauka", Novosibirsk, 1980.

25. Tylan Mass Flow Controller Operation and Service Manual, p. 8, Tylan Corporation, Torrance, CA.

26. Varian Variable Leak Valve, Model # 951-5100, Operating Instructions, p. 2, Varian Vacuum Division, Palo Alto, CA.

27. M.B. Panish, in "MBE of GaAs & InP with Gas Sources for As and P", Bell Labs, Murray Hill, NJ.

28. D.A. Stevenson, et al, in "Control of Impurities in the Epitaxial Growth of High Quality GaAs", Technical Report CMR-77-4, pp. 2,3.

Appendix A

Knudsen-Cell Effusion

A list of symbols pertaining to Knudsen cell effusion (equation 4 from the text) and their meanings follows:

$$\Phi = p/[2\ mkT]^{\frac{1}{2}}\pi \quad \text{molecules/cm}^2\text{-sec} \qquad (4)$$

Φ = flux out in molecules per cm^2 -sec

p = partial pressure-(1 atm = 1.013246×10^6 ergs/cm^3)

T = temperature in the cell

m = mass of the element- m = M(atomic wt. in amu)(1.65979×10^{-24}grams/amu)

k = 1.38062×10^{-16} ergs/°K

π = 3.1415927

An example calculation:

$$M_{Ga} = 69.72 \text{ amu} = 1.1572 \times 10^{-22} \text{ grams.}$$

$$[2\pi m_{Ga}k]^{\frac{1}{2}} = 6.33662 \times 10^{-19}$$

$$p = 1.31578 \times 10^{-14} \text{atm}[1.013246 \times 10^6 \text{ ergs-cm}^{-3}/\text{atm}] =$$

$$1 \text{ Torr} = 1.33322 \times 10^{-8} \text{ ergs/cm}^3 \quad (\text{or dynes/cm}^2)$$

$$\Phi = 13333.2184/[6.33662 \times 10^{-19}][T^{\frac{1}{2}}] = 2.10 \times 1021/T^{\frac{1}{2}} \text{ m/cm}^2\text{-sec}$$

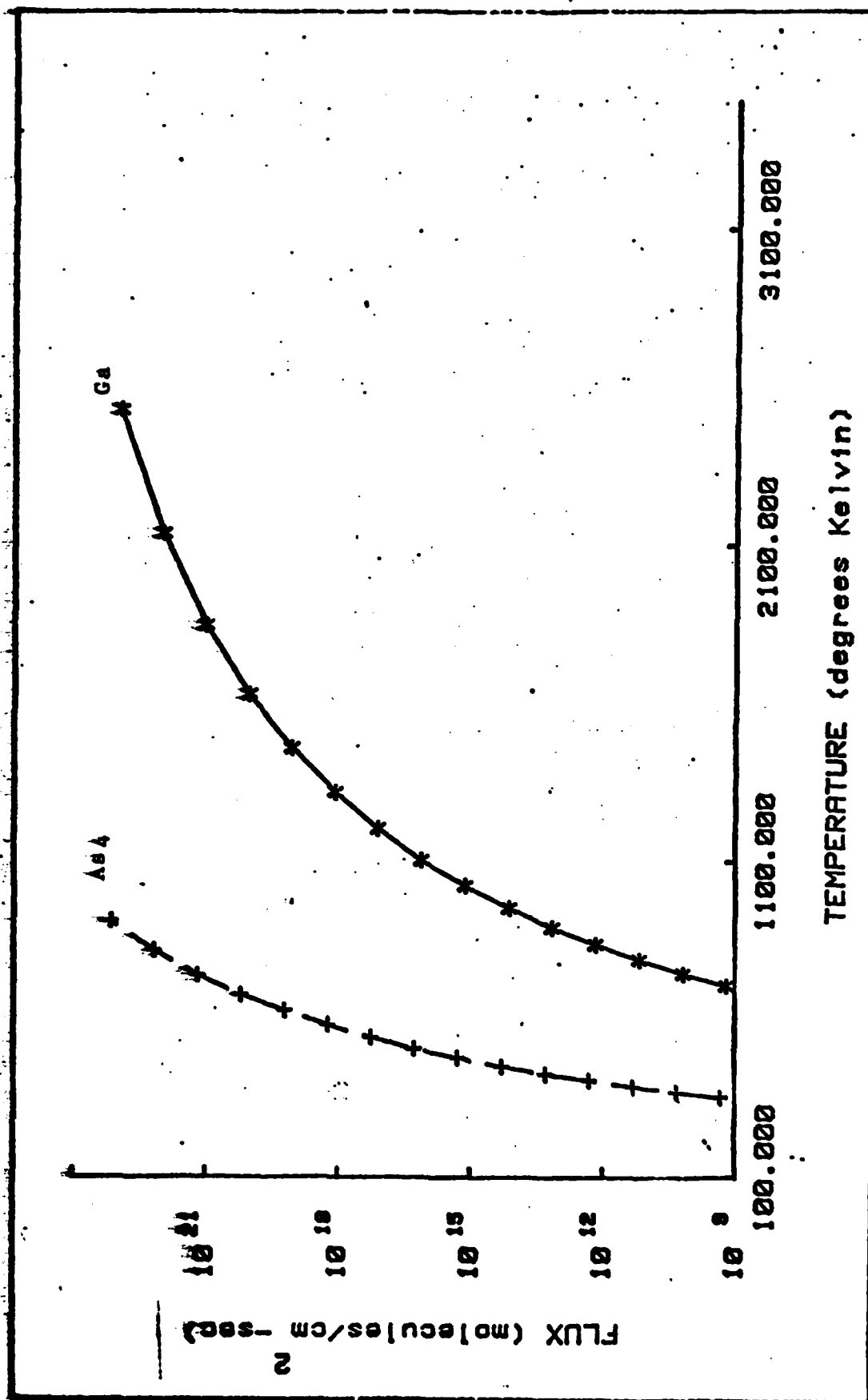See page 63 for plot of temperature vs. flux (Ref RCA Review June 1969, pp. 285-305).

Figure A-1 Knudsen Cell Effusion

Appendix B

Equations for Hall Measurements

<u>For the Hall-bar configuration the following equations are appropriate:</u>

$$\rho_n = 1/\sigma_n = E_x/j_{nx} = (V_x/x)/(I_x/yz) = V_x yz/I_x x \quad \text{ohm-cm} \tag{1}$$

$$\mu_{nH} = R_n \sigma_n = (E_y/[j_{nx}B/c])j_{nx}/E_x = (10^8/B)(V_y x/V_x y) \quad \text{cm}^2/\text{V-sec} \tag{2}$$

$$n_H = 1/R_n e = [j_{nx}B/c]/eE_y = 6.25 \times 10^{10} \, IB/V_y z \quad \text{cm}^{-3} \tag{3}$$

where x and y are defined in the figure below and z is the sample thickness. X,y and z are in cm. The final units are practical units, i.e. volts, (V), amps, (I), and B (gauss). R_n is the Hall coefficient, μ_{nH} is the mobility, σ is the conductivity, n_H is the density of the charge carriers, V_x is the Hall voltage, and the other symbols have their usual meanings.
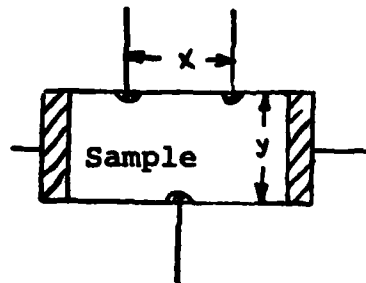
Appendix C

Calibration of Arsine Monitor

Dilute N$_2$ Liters/min	Tube Scale Reading	Standard AsH$_3$ (6 ppm)		Tube Scale Reading	Diluted AsH$_3$ (ppm)	Time to Respond
0	0	1		146	6	31 secs
0	0	1		146	6	25 secs
0	0	1	Set 1	146	6	27 secs
0	0	1		146	6	25 secs
.75	116	.25		56	1.5	63 secs
.75	116	.25	Set 2	56	1.5	67 secs
.75	116	.25		56	1.5	60 secs
.90	134	.10		35	0.6	106 secs
.90	134	.10	Set 3	35	0.6	112 secs
.90	134	.10		35	0.6	105 secs
.95	140	.05		21	0.3	296 secs
.95	140	.05	Set 4	21	0.3	277 secs
.95	140	.05		21	0.3	274 secs

Average Time to respond: Set 1 = 27 secs

Set 2 = 63 secs

Set 3 = 108 secs

Set 4 = 282 secs

Arsine Monitor first calibrated on 19 Aug 1982.

Appendix D

Detailed Emergency Procedures for Operation of Arsine Gas Manifold
And Cracking Furnace System with the MBE 360

Note: Two operators, who are thoroughly checked-out on the operation of the system, will always be present in the MBE Lab when Arsine is being used. One will be designated the Principal Operator (PO) and the other will be the Assistant Operator .

I. If the arsine monitor alarm sounds and there is no definite indication of a significant or massive arsine gas leak into the laboratory, the PO and AO will perform the following emergency procedures:

a. If not already wearing one of the Portable Breathing Units (PBU's) the PO and AO will go immediately to the MBE lab entrance and each will each quickly don one of the Scott-Air-Pak units (air tank, mask and regulator) which are located on the wall at the entrance to the lab, and will adjust these units for normal breathing conditions.

b. While wearing PBU's, the PO and AO will then order and direct the evacuation of all personnel from the immediate area of room D112 (the MBE lab and the VPE lab) and rooms 111 and 110. Personnel will be evacuated from the lab to a point of safety. (Preferred exit route is through D-Wing to E-Wing). If anyone in the lab is incapacitated for any reason, it will be the responsibility of the PO and AO to assist or carry such persons from the laboratory to a point of safety outside the lab and then to summon medical attention.

c. Once all personnel have been evacuated from the immediate area of room 112, the arsine system will be shut down. While still wearing PBU's, and with the AO standing by, the PO will move into the MBE lab, open the door on the secondary containment box (SCB) and turn off the main valve on the arsine bottle.

d. Once the arsine tank is turned off, and all other personnel have been evacuated from the area of room D112, the PO will attempt to determine the cause of the gas alarm and/or the origin of the arsine leak. The PO will, 1) clear and reset the arsine monitor (advance the tape drive and check the tape to insure it is functional, clean and not expended). If the monitor is functional, and if a second alarm sounds after resetting the monitor, the PO will, 2) purge the arsine manifold with high purity H_2, fed through the manifold and exiting through the arsine bleed line to the roof. (At this point the AO will check to see that all fume hoods and room exhaust fans in the lab are operating properly). The PO will, 3) again clear and reset the arsine monitor. If no alarm sounds, the area is clear of arsine and safe for the return of personnel. ·Personnel can be summoned to return to their work areas. If, on the other hand, a 3rd alarm sounds procedures of paragraph II will be followed.

II. If a massive arsine leak is known or suspected the PO and the AO will immediately evacuate all personnel in D-Wing. They shall alert the fire department by the fastest means available. If time permits the PO and AO will remove the portable breathing units from D-112, close and seal the door. Portable breathing units will be donned as soon as possible.

Appendix E

Characterization Analysis of Samples 196-

An analysis of sample 196 showed, in fact, that it was highly polycrystaline. Little or no nucleation was evident. Further analysis showed much the same results as sample 193, and therefore, the results are not repeated here.

Further samples were not grown with the cracking furnace as described in Chapter III. Modification of the helical furnace to include a tantalum wire along the center of the bore of the furnace, as suggested in Chapter V, showed a dramatic improvement in the efficiency of arsine cracking; and samples grown subsequently show good nucleation. But this is a subject for another thesis.

Vita

Gregory C. Clark was born on 8 November 1944 in Afton, Wyoming. He graduated from Davis High School, Kaysville, Utah, attended Weber State College in Ogden, Utah and Foothill Jr. College in Los Altos Hills, California, before serving two-and-a-half years in West Germany as a missionary for the LDS church. He graduated from Brigham Young University with a BA in Physics in 1969. As an NEA fellow he filled requirements for teaching physics and mathematics at the secondary level in 1970. He was commissioned a Second Lieutenant in the United States Air Force in May 1970. In June 1971, upon completion of USAF pilot training, he was sent to Mather AFB, Ca. Specializing in VIP airlift, he has also had assignments in Turkey (two years) and Germany (five years). He has accumulated over 3500 flying hours including over 1000 flying hrs. as a flight instructor and flight examiner in T-29, C-131, T-39, and VC-140B aircraft. He also served as headquarters squadron section commander for 16 months in Adana, Turkey, during which time, he completed requirements for a Master of Science degree in management from Troy State University. In June 1981, he entered the School of Engineering at the Air Force Institute of Technology, Wright-Patterson AFB, Ohio.

Permanent address: 521 Cheshire Way

Sunnyvale, CA 94087

REPORT DOCUMENTATION PAGE		READ INSTRUCTIONS BEFORE COMPLETING FORM
1. REPORT NUMBER AFIT/GEP/PH/82D-5	2. GOVT ACCESSION NO. AD-A124 676	3. RECIPIENT'S CATALOG NUMBER
4. TITLE (and Subtitle) USING ARSINE (AsH$_3$) AS A SOURCE OF ARSENIC IN MOLECULAR BEAM EPITAXY		5. TYPE OF REPORT & PERIOD COVERED MS Thesis
		6. PERFORMING ORG. REPORT NUMBER
7. AUTHOR(s) Gregory C. Clark Major		8. CONTRACT OR GRANT NUMBER(s)
9. PERFORMING ORGANIZATION NAME AND ADDRESS Air Force Institute of Technology (AFIT-EN) Wright-Patterson AFB, Ohio 45433		10. PROGRAM ELEMENT, PROJECT, TASK AREA & WORK UNIT NUMBERS Project 20020137
11. CONTROLLING OFFICE NAME AND ADDRESS Air Force Wright Aeronautical Laboratories Electronic Technology Division (AADR) Wright-Patterson AFB, OH 45433		12. REPORT DATE December 1982
		13. NUMBER OF PAGES 79
14. MONITORING AGENCY NAME & ADDRESS(if different from Controlling Office)		15. SECURITY CLASS. (of this report) Unclassified
		15a. DECLASSIFICATION/DOWNGRADING SCHEDULE

16. DISTRIBUTION STATEMENT (of this Report)

Approved for public release; distribution unlimited

17. DISTRIBUTION STATEMENT (of the abstract entered in Block 20, if different from Report)

18. SUPPLEMENTARY NOTES

Approved for public release: IAW AFR 190-17.

LYNN E. WOLAVER
Dean for Research and Professional Development
Air Force Institute of Technology (AIC)
Wright-Patterson AFB OH 45433

19 JAN 1983

19. KEY WORDS (Continue on reverse side if necessary and identify by block number)

Molecular Beam Epitaxy
Arsine
Gallium-arsenide
Arsine Cracking

20. ABSTRACT (Continue on reverse side if necessary and identify by block number)

Recent research indicates that cracked arsine produces a better source of As than the conventional solid sources for the MBE growth of quality semi-conductors. Further investigation into this topic was the problem of this thesis. A Varian 360 MBE system with conventional furnaces was modified for use with arsine. An Arsine handling system and two different cracking furnaces using commerically available resources were constructed. The first furnace constructed was a bulbous design with internal baffles for insuring

DD $_{1\ JAN\ 73}^{FORM}$ 1473   EDITION OF 1 NOV 65 IS OBSOLETE

longer dwell times for the arsine molecules. The second design used a helical quartz tube, approximately 20 inches long, inside a tantalum furnace. Several samples were grown using each cracking furnace. Prelinimary results indicate an unsuspected cracking mechanism is responsible for earlier successes; perhaps the primary cracking mechanism is not pyrolytic but photolytic or catalytic.

products of arsine cracking. Calawa indicates in his work that the dimer and the tetramer are present in significant amounts when arsine is cracked. He speculates that recombination may be responsible for the high levels of these species. We found no trace of either As_2 or As_4 with the first cracking furnace. The second furnace did show a small trace of As_2, but only by using the very highest gain level (10^{-12}) of the PGA. Figure 5-1 is an oscilloscope trace which shows the presence the As_2 species. No trace of As_4 was ever detected. This result is surprising, and demonstrates again that the cracking mechanisms are poorly understood at present.

Perhaps a laser could be used to investigate AsH_3 cracking under UHV conditions, in a manner similar to the method described in reference 19, where a laser operating at 193 nm is used to dissociate arsine. A primary difficulty is the small molecular cross section of each species under UHV conditions.

58

END